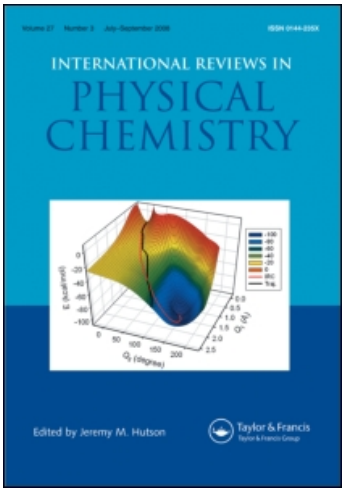

International Reviews in Physical Chemistry
Publication details, including instructions for authors and subscription information:
http://www.informaworld.com/smpp/title~content=t713724383

Cryochemical chain reactions

I. M. Barkalov; D. P. Kiryukhin

Online publication date: 26 November 2010

To cite this Article Barkalov, I. M. and Kiryukhin, D. P.(2000) 'Cryochemical chain reactions', International Reviews in Physical Chemistry, 19: 1, 1 — 43
To link to this Article: DOI: 10.1080/014423500229846
URL: http://dx.doi.org/10.1080/014423500229846

INT. REVIEWS IN PHYSICAL CHEMISTRY, 2000, VOL. 19, NO. 1, 1–43

Cryochemical chain reactions

I. M. BARKALOV† and D. P. KIRYUKHIN
Institute of Problems of Chemical Physics, Russian Academy of Sciences, Chernogolovka, Moscow Region, 142432 Russia

The possibility of a chemical reaction near absolute zero has appeared doubtful since the beginning of the 1970s. The existing ideas must be revised after the radiation polymerization of formaldehyde at 4.2 K has been observed. In glassy systems, we have examined chain processes that occur under sharp (by five to six orders) changes in molecular mobility of the medium in the region of matrix devitrification. Quite unusual mechano-energetic chains of chemical conversion arise in the studied systems submerged in liquid helium. The chemical transformation initiated by local brittle fracture travels over the sample as an autowave. A series of experimental and theoretical investigations devoted to this interesting phenomenon are described. There is no generalization in this new region of chemistry up to this time. Many journal articles and reviews have been previously published only in Russian. The cycles of investigations of chain cryochemical reactions are the subject of this review. We hope that the investigation of the extraordinary peculiarities of chain cryochemical reactions should produce new ideas in chemical theory and industry.

1. Introduction

Most researchers who study the chemistry of high-activity intermediates often call this field of knowledge simply 'cryochemistry'. That is the reason why we have emphasized the word 'chain' in the title of our article, that is the processes in which the object affected by small perturbations (e.g. by liberation of a stabilized intermediate) gives a chain of chemical conversions occurring spontaneously.

More than 20 years ago, starting a cycle of investigations into chain cryochemical reaction, we understood that we were becoming involved in the study of the unusual, and we are sure that that holds true up to the present. The traditional theory of chemical reaction (the necessity to surmount an activation barrier) and the experience of a thousand years of mankind have convinced us that cold kills all composite chemical conversions. On the other hand, almost half the substance in the Universe exists under the conditions of cosmic cold.

The aim of this review is to produce experimental evidence of different ways of principle chemical conversions under low temperatures and weak radiation fields.

The classical picture of an elementary act of chemical transformation is based on the following postulates.

(1) The necessity of surmounting the activation barrier in the interaction of reactants exists.
(2) The energy necessity for surmounting the activation barrier is received by chemical reactants from intermolecular interactions.

† Email: barkalov@icp.ac.ru.

International Reviews in Physical Chemistry ISSN 0144-235X print/ISSN 1366-591X online © 2000 Taylor & Francis Ltd
http://www.tandf.co.uk/journals/tf/0144235X.html

(3) The time necessary for accumulation of this energy by the reactants (characteristic time of an elementary act) is determined by the temperature of medium.

It is easy to show that these postulates exclude completely the possibility of chemical conversion near the absolute zero.

It was difficult to imagine an effective chemical conversion that took place without considerable transfer of masses of reagents and products. Nature seems to carry out chemical reactions in solids only on the geological time scale and even then liquid and gas phases, mechanical destruction, and high pressures and temperatures are present. Combustion of solid fuels, detonation of explosives, and the processes of burning and caking were always considered as reactions at the surface of contact between the solid phase and gas or liquid.

The new ideas about the mechanism of an elementary act of chemical reaction near absolute zero now actively discussed do not touch on the problem of the mechanism of the *chain* reaction process. Together with the question of the mechanism of surmounting the activation barrier between reactants, which needs to be answered, there is also a question of the mechanism of reactants shifting in each act of association. This crucially important question is left open.

There arises a paradoxical situation: most of the important industrial processes, for example ammonia syntheses from elements, are thermodynamically advantageous if carried out at the lowest possible temperatures, while they are actually carried out at high temperatures. The transfer to low temperatures is advantageous also because the decrease in the temperature of complicated chemical syntheses leads to a distinctive selection between various channels of conversion; only these reactions 'survive' that have the lowest activation energy.

As early as the 1930s, some work that reported on polymerization in crystal monomers appeared. Crystalline trioxane in the presence of formaldehyde vapours polymerized to form polyoxymethylene fibres oriented along one of the crystallographic axes [1]. Later the formation of rubber-like polymers of acetaldehyde at the moment of freezing (crystallization) or melting was discovered [2, 3]. It was already a transition to low temperatures. It appears that, in spite of the difficulties, effective chain reactions can occur at the same time in a solid and at low temperatures.

The concepts about the impossibility of the occurrence of chemical reactions near absolute zero were rejected after a new phenomenon was experimentally established, that of the low-temperature limit of the rate of chemical reaction. This phenomenon was discovered when studying the mechanism of solid formaldehyde polymerization in the temperature range 4–100 K [4]. Then the existence of the low-temperature reaction rate limit was discovered for a number of chain and non-chain chemical reactions [5]. There are some chemical reactions that take place at the temperature of liquid helium with a rate which, although it is low, is quite measurable and independent of the temperature. Immediately after the discovery of the phenomenon of the low-temperature rate limit it was suggested that its mechanism could be interpreted according to the concept of molecular tunnelling. This idea was developed, taking into consideration molecular vibrations [5–9].

Regardless of the difficulties, it turns out that effective chain reactions can occur in solids and at low temperature as well. Therefore, where is the energy necessary for surmounting the activation barrier of a chemical reaction and mass transfer of reactants and products taken from?

The mechanical energy of elastic deformation at the instant of fracture is concentrated in the region immediately near the surface being formed. It is known that the process of energy transformation is accompanied by a significant change in the physicochemical properties of the substances on the newly formed surface from those in the bulk; brittle fracture is connected with such phenomena as electron and ion emission, luminescence, radical formation, and dramatic acceleration of the transfer processes on fracture surfaces.

In other words, it seems probable that switching the process over from the homogeneous regime to the essentially heterogeneous state would switch on the non-equilibrium mechanism of energy transfer to active centres pre-frozen in a three-dimensional matrix and would thereby cause a chemical conversion at such low temperatures.

Our investigations lead to the observation of highly intense autowave regimes in low-temperature solid-phase reactions. The principal conclusions have been surveyed in the reviews given in [10, 11]. On local brittle fracture of a sufficiently long sample of reactants a chemical reaction starts on a newly formed surface. The temperature or density gradients arising during the reaction lead to further layer-by-layer dispersion of the solid sample. Because of this positive feedback an autowave of chemical conversion spreads over the sample. Such an autowave regime is observed for a whole series of reactions (hydrocarbon chlorination, olefin hydrobromination, and polymerization) at 4–77 K. This concept has allowed us to create new ideas of autowave mechanisms of cold chemical evolution in the Universe.

2. The cryochemical chain reactions in crystals

2.1. *Solid-phase polymerization of formaldehyde*

In the 1960s a rapid development of investigation into solid-phase polymerization took place. However, most of these studies were of a phenomenological nature and the theoretical conclusions and hypotheses were more hypothetically than experimentally founded. It seemed at first that strict orientation of monomer molecules in space characteristic of crystals could affect the regularity of the forming macromolecules. Moreover, there appeared hopes that 'orderly army ranks' of reactants in a crystal would favour faster transformations. As early as 1960, Semenov [12] suggested a mechanism of high-energy chains for the processes of solid-phase polymerization [12]. The idea was that the energy evolved in each elementary act of polymer chain propagation did not disperse, transforming into heat, but, owing to a collective interaction of a monomer 'stock' in a crystal, ensured surmounting the activation barrier in the next such act. The movement of an exciton along the 'stock' was assumed to be one of the variants of such a collective interaction. Then polymer chain propagation might occur in the same way as an exciton spreading [13].

We shall not discuss the extensive factual material collected to date; the reader can become acquainted with this in [12, 14–19]. We shall give only the major conclusions from this period. A transfer of a monomer crystal into a polymer is connected with changing both the average distances between separate fragments (intermolecular distances are replaced by chemical bond lengths) and the spatial orientation of the monomer links. There are two extreme cases: firstly the structure of a monomer crystal significantly determines the polymer structure (derivatives of conjugated diacetylenes, and trioxane) and secondly, a polymer arises as a separate phase, in the extended lattice defects, which leads to further destruction of the monomer crystal. The polymeric phase is amorphous (acrylamide). Many intermediate cases exist. The

transfer of the classical concepts of the mechanism of reactions in gaseous and liquid phases to the solid-phase process appeared to be fruitless and new ideas were required.

Because of the low probability of translations in a crystal it is difficult to imagine the decay of growing macroradicals through recombination or disproportionation. The process of propagation of a polymer chain gradually comes to an end owing to the progressively increasing difficulties in the access of monomers to a growing active centre; a kinetic halt to the process is observed ('setting and reviving' of a polymer chain [20]), which has led to developing the idea of 'polychronous kinetics' [21].

A series of investigations was performed on the mechanism of chain cryochemical reactions (polymerization and hydrobromination) that effectively continued near the absolute zero of temperature. The investigation of radiation polymerization of formaldehyde at 4.2 K allowed us to discover the phenomenon of the low-temperature limit of the rate of chemical reactions. The existence of this phenomenon was subsequently established for a number of other chain and non-chain reactions. The rates of their reactions were not dependent on the temperature. The main results of the study of solid-phase formaldehyde polymerization in the range 5–150 K were given in [22–29].

In an example of solid-phase formaldehyde polymerization, it was first experimentally demonstrated that a chain reaction could proceed near absolute zero. It also appeared that in the range 77–140 K the temperature dependence of rate was satisfactorily described by the Arrhenius law. However, at lower temperatures, the chain propagation gradually decreased and beginning with $T \approx 15$ K it ceased to be temperature dependent, i.e. the *low-temperature limit of the chemical reaction rate*. Here $\tau_0 \approx 0.01$ s, while extrapolation using the Arrhenius law with an activation energy would have given $\tau_0 \approx 10^{30}$ years even at 10 K!

The polymerization of formaldehyde is a chemical reaction in the true sense of the word; a row of planar triangular monomer molecules transforms into long chain of tetrahedral bonds, $-O-C-O-$. Replacements of the van der Waals radii of the carbon and oxygen atoms in the monomer by shorter valence bonds, C—O, lead to a significant (about 40%) increase in the density of the substance.

2.2. *Solid-phase ethylene hydrobromination*

In our further search, we turned to the chain reactions of addition in multiple bonds, for example to ethylene hydrobromination. The photochemical hydrobromination of olefins at $T = 77$ K was described in detail in [30, 31]. We carried out work on the dynamics and mechanism of radiation-induced hydrobromination of ethylene in the temperature range 30–90 K [32, 33].

Thus the reaction of radiation-induced hydrobromination of ethylene in the solid phase is one more example, together with the chain reaction of formaldehyde polymerization, of the low-temperature limit of the chemical reaction rate. A comparison of the rate constants of chain propagation in hydrobromination in the deuterated systems shows that hydrogen transfer cannot be a limiting stage of the process at low temperatures.

We should take into account not only the 'pure' tunnelling of heavy particles through the activation barrier but also the participation of intermolecular movements of reactants in the crystal lattice to understand the phenomenon of the low-temperature rate limit of chemical reactions.

2.3. *Cryochemistry of hydrogen cyanide*

The molecular formation of hydrogen cyanide (HCN) is very abundant in cosmic space: in gigantic clouds of comets, protoplanet clouds, interstellar dust and other galactic structures. In general, the HCN molecule is commonly considered to be the basis of pre-biological chemical evolution, since its transformations provide a direct pathway to purines, pyrimidines and amino acids [34–38]. Stahler [39] suggested that the length of the chain of cyanopolyene macromolecules that arise upon condensation of HCN may be used as an inherent clock for determining the age of interstellar clouds. Astrophysical aspects of the chemical transformation of HCN are being intensively studied [40, 41].

It is of interest to study the chemical behaviour of this simple molecule under conditions similar to those in outer space (low temperatures and radiation) and its role in the 'cold' chemical evolution of the Universe. We present below the fundamental results of a number of experiments carried out along this line in recent years [42–44].

When HCN is cooled to 77 K, it transforms to a crystalline state. During its heating, a phase transition of the crystal–crystal type (248 K) and melting occurs at 260 K ($\Delta H = 8.4 \pm 4$ kJ mol^{-1}). Calorimetric measurements carried out directly in the irradiation field at 77 K show that there is no noticeable heat evolution associated with chain polymerization. When HCN after irradiation at 77 K is warmed to room temperature, the formation of a polymer occurs. The thermal effect of the polymerization of HCN is recorded only for melting. The yield of the polymer formed during heating the HCN specimens irradiated at 77 K to ambient temperature increases, as the dose of preliminary irradiation is increased, and reaches 2.5% for the dose equal to 725 kGy. It is of interest that the radiation-induced polymerization of liquid HCN at 273 K occurs much less efficiently.

Prolonged storage of HCN in a sealed evacuated cell at room temperature does not result in any changes in its colour and formation of polymeric products. At the same time, when HCN samples after irradiation at 77 K are kept at room temperature, their colour is changed (from light brown to almost black), and polymeric products are formed. The polymerization yield increases with increasing time of storage and is as high as 33.5% after 750 h.

The analysis of the infrared (IR) absorption spectrum of the freshly prepared polymer has shown that, together with the absorption bands due to C≡N stretching vibration (2100–2200 cm^{-1}) that have also been observed in the spectrum of the monomer HCN, this spectrum exhibits additional bands at 1600–1700 cm^{-1} and 1200–1250 cm^{-1}, which are apparently caused by stretching vibrations of the C=N and C−N bonds respectively. When the system is kept at room temperature, structuration of the polymeric product occurs, together with an increase in its amount. In the IR absorption spectrum, redistribution of the intensities of the bands at 1250 and 2200 cm^{-1} and an increase in the background in the region 1700–2200 cm^{-1} occur, although all the basic absorption bands remain unchanged.

The polymer exhibits a singlet electron spin resonance (ESR) spectrum characteristic of polyconjugated systems. The electrical conductivity of this polymer is typical of most dielectrics. Colouring of the polymeric product and deepening of its colour (up to black) during the process can be more reasonably explained with the radical scheme of the transformation as resulting from the formation of the C=N−C=N− conjugated chain.

The formation of needle crystals of the HCN tetramer may be due to recombination of two biradicals which gives a tetramer, 1,2-diaminomaleinodinitrile [43]:

$$N\equiv C-C-NH_2$$
$$\|$$
$$N\equiv C-C-NH_2$$

In fact, photolysis of a glassy solution of a lithium salt of 1-cyanoformamide-*p*-toluenesulphonyl hydrazone in 2-methyltetrahydrofuran at 77 K results in the formation of a yellow product, aminocyanocarbene [45]. An $H_2N-C-C=N$ biradical is in the singlet state. Dimerization of aminocyanocarbene lead to a tetramer of HCN [46]. Those noticeable amounts of the tetramer formed in our experiments on radiation polymerization makes it possible to suggest that the above-described mechanism is realized. Aminocyanocarbene is likely to initiate the subsequent growth of the chain of HCN polymerization, leading to the formation of a polymeric product. It cannot be ruled out that it is aminocyanocarbene that plays a key role in the pre-biotic organic synthesis.

First, we ought to demonstrate that the tetramer crystals arise in the solid state, during the unfreezing of HCN radiolysed at 77 K, or after its melting. In this connection, we carried out the reaction in the following way. After irradiation of solid HCN, we placed it in a vacuum and carried out the sublimation of the unreacted monomer at a temperature below the melting point (260 K). The residue obtained after this prolonged sublimation (2.5% of the initial weight) was a mixture of the polymer and the crystalline tetramer. It is of fundamental importance that these products were formed in the solid state.

An X-ray structural investigation of crystals taken from the residue of the above-described sublimation has shown that these crystals are of monoclinic syngony [44]. The bond lengths and angles are conventional. The molecule is planar and has its own symmetry plan, $C\equiv N$ triple bonds and $C=N$ double bonds are localized. There are no shortened intermolecular contacts or other specific interactions in the crystal.

Thus, it has been experimentally shown that, during the sublimation of a solid HCN matrix irradiated at 77 K, together with the conjugated polymer of the $-[C=N-C=N]_n-$ type, crystals of 1,2-diaminomaleinodinitrile are formed. These crystals are produced by the recombination of biradicals of the aminocyanocarbene type, which are stabilized by the low-temperature radiolysis of the matrix. During the sublimation of the matrix near its melting point, these biradicals acquire molecular mobility and recombine.

1,2-Diaminomaleinodinitrile has been formed in our runs in a radiation yield $G \approx 2$ (molecules in a gram per 100 eV of the absorbed energy). This radiation yield is normal for the products of primary radiation transformation (e.g. radicals). Therefore, 1,2-diaminomaleinodinitrile cannot result from consecutive radiation reactions. We suggest that HCN exists as a dimer in the solid matrix owing to the hydrogen bonds with $C\equiv N$ groups. The primary readiation excitation of these dimers results in the appearance of aminocyanocarbene. Somehow, this 1,2-diaminomaleinodinitrile is formed under conditions close to those in outer space (low temperatures and radiation), which seems to be of considerable importance, since this compound might have played a key role in the pre-biological organic synthesis, because hydrolysis of 1,2-diaminomaleinodinitrile directly leads to an amino acid. Polymerization of the closest analogue of HCN, dicyane ($(CN)_2$), is of no less interest from the viewpoint of cold chemical evolution of substance in outer space and formation of complex polymeric molecules.

2.4. *Conclusion*

Thus the years of laborious investigations and experimental search have compelled us to believe that the formation of complex chemical compounds through a long chain of chemical conversions is possible at temperatures close to the absolute zero. This provides evidence for the possibility of formation of complex bricks of living nature in the cold space of the Universe.

Unfortunately, it is necessary to state that during this year there were many more theoretical considerations of the possible mechanisms of such reactions than actual experimental work that could serve as a basis for the selection of hypothetical mechanisms. At present the situation in this field is as follows: there are a number of systems for which the fact of a chemical reaction occurring at temperatures close to the temperature of liquid helium is established. However, the study of the dynamics of the chemical process (the main foundation of a theoretical construction) is carried out only in exceptional cases. There is unfortunately no unambiguous experimental answer to the question: where is the energy needed to surmount a barrier taken acquired from or is the barrier in fact absent?

Also, it is quite obvious that together with the thermal activation prohibited at such a low temperature, there is the possibility of introducing the energy into the system during initiation. The processes of self-regulation are also possible because of the mechanical energy accumulated and produced in the chemical reaction. The existence of such alternatives has intensified in recent times the demands for the quality and amount of experimental information sharply reduced by the scarce and outdated experimental devices.

After reading section 3, the reader will be convinced that the number of the systems where chemical conversions near absolute zero take place has been markedly extended. We have found that there are actually existing mechanisms in which the energy of chemical conversion is automatically used to develop the process. Thus, what are the causes of the chain chemical conversions that take place under the conditions of cosmic cold? Are these the quantum effects in the elementary act or peculiar self-regulating mechanisms?

3. The cryochemical chain reactions during glass devitrification

In amorphous bodies, the three-dimensional periodicity of the structure, that is the main characteristic of the crystal state, is absent. However, there is short-range order in an amorphous body, when the mutual arrangement of several molecules is intercorrelated. Because of the absence of long-range order, amorphous bodies are isotropic; their macroscopic properties do not depend on the direction. At temperatures above the melting point T_m the substance passes to another equilibrium state, namely a crystal state. However, upon sufficiently fast cooling, the state of a non-equilibrium overcooled liquid is reached. Further cooling of this state down to below the vitrification point T_v leads also to the non-equilibrium solid amorphous state, often called merely a 'glass'. The vitrification point is rather an inappropriate name, although commonly accepted. In fact, the transition from an overcooled liquid to the glass state occurs usually in a narrow temperature interval. The glass point T_g itself is not a thermodynamic characteristic of the substance and may vary in a wide range depending on the conditions of measurements that are connected with a sharp retardation of the structure rearrangement in the short-range order of a liquid. In the glass state the particles can make only vibrational and small-scale rotational

movements. Translational mobility, characteristic of the liquid state, is almost lost here.

Although the vitrified state of the substance is metastable (the specific volume and enthalpy of glass are higher than those of an equilibrium crystal), it can survive for a long period of time. Such natural glasses as obsidian and amber exist for millions of years. The theoretical description of the glass state markedly lags behind the modern theory of crystals. The requirements of practice (fibrous optics and metallic glasses) have particularly intensified the efforts of physicists and there is hope that theoretical efforts will make it possible to overtake the far-advanced experimentalists.

It is also very important that the transition from an supercooled liquid to the glass state or a back transition (devitrification) is followed by a sharp change in the properties; *the viscosity is changed* (*by ten to 15 orders*), as also are the elasticity modulus and temperature expansion coefficient. The most impressive here is of course the gigantic jump in viscosity in the narrow temperature range of devitrification. For a chemist it is clear that the molecular mobility determining the dynamics of chemical conversion changes sharply in this region. We are used to the fact that the dynamics of the process (of course, without catalysis) can vary only because of the temperature of the medium in which the chemical reaction occurs. The temperature dependence of the chemical reaction rate has become very familiar: $K = Z\exp(-E/RT)$. Thus the character of the chemical process is not described by this traditional equation in the region of glass softening and should change drastically owing to rather a sharp change in the mobility of the reactants. Meanwhile, a great change in the mobility of molecules is reached by temperature variations of a few degrees. The next section is devoted to the first steps in the study of these unusual chemical processes.

3.1. *Radical polymerization*

As early as 1962 it was shown that vinyl acetate can be polymerized in both the glass and the crystalline states. The polymerization rate for glass vinyl acetate under similar conditions appeared to be an order of magnitude higher than for crystalline vinyl acetate [47]. High rates of post-radiation polymerization were detected for a series of glass solutions of monomers in paraffin oil and other glass-forming solutions [48, 49]. However, a significant drawback of all the early work was the use of a traditional gravimetric techniques for determination of the polymer yield and, hence, the polymerization rate. The polymer yield in the devitrification region was estimated, for instance, by measurements at room temperature after destruction of the matrix. To perform quantitative kinetic measurements, it was necessary, at first, to create techniques that could allow us to control the process directly at the moment of its occurrence. In every particular case it was also necessary to perform a phase analysis of the two-component system 'reactant–vitrifying matrix' to determine the limits of solubility at vitrifying temperatures of the system and, finally, in the vitrifying temperature region itself. Further successes in the study of the chain reaction mechanism in matrix devitrification were connected with the development and use of kinetic calorimetry that successfully solved the above experimental tasks.

The use of calorimetric technique allowed us to establish that the polymerization in a series of radiolysed glass systems proceeded on their defreezing in the temperature range of matrix devitrification [50–52].

Let us consider in more detail the polymerization in the acrylic acid–ethanol glass system [53]. A 17% acrylic acid solution in ethanol was established to change completely to the glass state on freezing down to 77 K. As this glass was defrozen in

the calorimeter, the system passed to an overcooled liquid state with $T_g \leqslant 103$ K. The latter, on further heating, changed to the thermodynamically stable liquid region (without crystallization and subsequent melting). Direct calorimetric measurements in the γ-ray field showed that no polymerization took place in this system at $T \leqslant T_g$. The calorimetric curve produced in defreezing a radiolysed glass solution showed intensive heat release just after the sample softening, which was connected with the polymerization of acrylic acid. The total polymer yield here reached 80%.

In accordance with the ESR spectra at $T \geqslant 108$ K a transition of monomeric radicals and radicals of an alcoholic matrix formed in radiolysis into the radicals of a propagating polymer chain $R-C_\beta H_2-C_\alpha H-COOH$ took place. A detailed analysis of evolution of ESR spectra of these radicals and their conformational conversions was made in [54]. Together with the initiation of the polymer chain, recombination of a part of the monomer radicals took place, nearly half of them turning into propagating polymer radicals. On further heating, in the temperature range where polymerization of acrylic acid proceeded intensively, the concentration of growing polymer radicals remained constant. A more recent study of the polymerization dynamics in this system by the Mössbauer labelling technique (ferrocene 0.4 wt%, enriched by 90% by isotope ^{57}Fe) confirmed the correctness of the main conclusions [55].

Therefore, in a rather narrow temperature interval in the matrix devitrification region, the polymerization continues almost without chain termination. The radicals stabilized in glass during radiolysis acquire a translation mobility while passing through the devitrification region and begin to recombine. Simultaneously the reaction of the addition of radicals in the double monomer bond occurs. The growing radicals are formed, whose mobility in a viscous overcooled liquid is so small that their collision and recombination are almost not observed. Meanwhile, a supply of small monomer molecules to such growing centres occurs readily, and their growth is continued. This unique situation, as will be clear from the following, is widely used in various polymerization processes.

3.2. *Chain transfer*

Thus, intensive polymerization is observed in the process of defreezing glass monomers during its transition to the state of viscous supercooled liquid. The characteristics of this process are the long (in comparison with a usual liquid) times of the mutual contact of reagents and the absence of termination of propagating polymer chains in a certain temperature range. It seems likely that, under such conditions, polymer products with rather high molecular masses should form. In reality, this is not observed. We may suppose that even at these low temperatures the reaction of chain transfer through a monomer or solvent may play a marked role, limiting the polymer chain length owing to the long time of mutual contact of reagents. The chain transfer is thought to be a reaction of, for instance, the detachment of hydrogen from the monomer or solvent by a propagating macroradical to form an inert macromolecule and a radical initiating propagation of a new polymer chain.

The study of polymerization on devitrification of radiolysed glass solutions of acrylic acid, acrylamide and methylacrylate in ethanol was given in [56]. If the stage of chain transfer plays an important role in the polymerization process, then the average length of a kinetic chain will be sufficiently greater than the average length of a polymer chain. As has been stated above, the ESR method allows us to measure directly the concentration of propagating polymer radicals for the systems in question.

Therefore, knowing the polymer yield and the number of propagating macroradicals it is easy to determine the average length P_k of a kinetic chain. This value should be compared with the average length P_p of a polymer chain obtained by viscosimetric measurements of the molecular mass for the polymers produced. It was found that, in the case of acrylamide polymerization, P_k is 100 P_p. Such an inconsistency can be understood only in terms of an effective chain transfer.

Therefore, the destruction of polymer chain in a narrow temperature range is absent in the process of polymerization during devitrification, and the chain transfer can also proceed effectively there. In fact, there is report of a remarkably sensitive system with kinetic chains of not less than 10^7 [57]. This is a glass solution of acrylamide in glycerine. When this solution, radiolysed at 77 K, is being defrozen, the transition from a glass to an overcooled liquid is observed at $T_g \approx 190$ K. The subsequently effective monomer polymerization proceeds in the temperature range 220–260 K. An extremely small dose of irradiation, about 0.3 Gy, is needed for polymerization of this system. The polymer yield has been calculated by calorimetric measurements and by the amount of the polymer produced in the reaction. The difference between these two methods of yield determination is not more then $\pm$ 5%.

We have used an ESR technique to record the number of propagating polymer radicals and to calculate their radiation–chemical yield. The system has been found to form about 0.6 ± 0.2 macroradicals per 100 eV accumulated energy. Therefore, the kinetic chain length is 10^7, that is one act of chain generation leads to conversion of more than 10^7 monomer molecules. We do not know any other polymerization processes even at room temperature that are so sensitive to initiating radiation.

3.3. *Ionic polymerization*

A sharp change in the matrix physical properties in the transition through the devitrification region affects the dynamics of polymer chain development by the cationic or anionic mechanism. As the low-temperature radiolysis in glasses leads to stabilization of not only radicals but also captured electrons and holes, the possibility for the reaction to proceed by the ionic or by the radical mechanism seems to be the same. Here we should mention briefly the history of the study of radiation-induced polymerization by the ionic mechanism. There is evidently nothing to prevent the examination of this process, since it is the ions that are the main initial products of the radiolysis. However, by the time when the radiation polymerization by the radical mechanism had been already extensively studied, ionic radiation-induced polymerization in the liquid phase at room temperature had failed to be obtained. Many painstaking efforts were needed to understand that the water traces in monomers and solvents were the strongest inhibitors of this process. The application of complicated techniques of preliminary drying of reagents led finally to success.

We might suppose that in a post-polymerization regime about the matrix devitrification no special methods of drying the monomer and solvent were required as the polymerization proceeded at quite low temperatures. In this temperature region, the lifetime of ions increased, and the water traces were isolated in their own crystal phase and could not inhibit the polymerization.

Heating of γ-irradiated (at 77 K) glass solution of cyclopentadiene (20%) in butyl chloride results in an effective monomer polymerization [58, 59]. The heat release connected with cyclopentadiene polymerization is observed in a narrow temperature region just after the transition of the system from a glass to an overcooled liquid. Thus the use of the post-polymerization method in matrix devitrification allows one to carry

out an effective cationic polymerization of cyclopentadiene. The peculiarity of this process is the absence of any special requirements to drying of a monomer and a solvent.

Ethylene oxide is readily polymerized with opening of the epoxy cycle by the cationic or anionic mechanism in the presence of a large number of catalysts. However, the epoxy cycle appears to be rather stable to the action of high-energy radiations. The attempts to carry out radiation polymerization of ethylene oxide in the solid and liquid phases proved unsuccessful and led only to formation of polymer traces, while the radiation yield of monomer molecules consumption for polymer formation did not exceed $G(-M) \approx 10$ [60]. A radiation-initiated effective polymerization of ethylene turned out well using a post-polymerization regime in devitrification of the butyl chloride matrix [59, 61].

As distinct from a crystal monomer, heating of γ-irradiated (at 77 K) glass solutions of ethylene oxide in butyl chloride leads to an effective polymerization. The heat release connected with the ethylene oxide post-polymerization occurs in the temperature range of glass softening at about 96 K. Thus, as distinct from other radiation polymerization techniques for ethylene oxide, the use of a post-polymerization method in matrix devitrification makes it possible to carry out an effective polymerization of ethylene oxide with opening of the epoxy cycle. The post-polymerization proceeds by the cationic mechanism and does not require any special methods for drying the monomer and solvent.

Therefore, polymerization by the ionic mechanism and radical polymerization in devitrification proceed in a certain temperature range without chain termination. In the case of the ionic mechanism, however, this temperature interval is even narrower, as the process is only limited by defreezing of the matrix molecular mobility.

3.4. *Chlorination of saturated hydrocarbons*

Chain chlorination of paraffin hydrocarbons and their chloro derivatives in the gas and liquid phase in photo and radiation initiation was studied in every detail [62]. However, none of these investigations obtained the specificities of the processes in solid and viscous media. It appears that the specific characteristics of the chain process in matrix devitrification demonstrated above are qualitatively preserved for reactions such as the chlorination of paraffins.

The specificity of low-temperature radiation chlorination in glass matrices was studied for the system butyl chloride–molecular chlorine [63]. Dissolution of molecular chlorine in butyl chloride is performed in the dark at 180 K, and no chemical reaction proceeds at that time. This solution also transforms to the glass state on freezing. The simplest picture of phase conversions is observed for the solution with the ratio of 1 mol of chlorine per 3 mol of butyl chloride. This solution does not crystallize after devitrification and, hence, does not melt. Therefore, there is no phase separation at such ratios in a vitrifying solution. This is quite important since, in the case of a homogeneous one-phase system, the interpretation of kinetic data is simplified significantly.

Thus, just as in the case of polymerization, the chain reaction of the chlorination of chloroparaffins in the supercooled liquid is characterized by the long lifetime of the active centres. With a temperature increase in an overcooled liquid the propagation rate reaches a maximum and, when the system passes to a thermodynamically stable liquid and the viscosity of the medium drops sharply, the probability of chain

termination rises. So we may conclude that suppression of chain termination while simultaneously ensuring an effective propagation of the chains (the regime that is automatically realized near the devitrification region of the system) makes it possible to increase the total reaction rate.

3.5. *Hydrobromination of olefins*

Photochemical hydrobromination of olefins at low temperatures has been described [30, 64], and we have carried out investigations into radiation ethylene hydrobromination at 30–90 K [32, 33, 65]. This is a second example (after formaldehyde polymerization) of the phenomenon of the velocity limit to chain chemical reactions. In [42] the phase condition of the system allyl chloride (AC) + HBr was the dynamics of spontaneous and radiation-induced hydrobrominating in the temperature range 77–200 K were studied. A known amount of AC and HBr was frozen in a previously evacuated calorimetric cell to prepare a sample of AC + HBr. The cell was then sealed. Next the sample was heated so that the reactants could transform to the liquid state but not above 180 K in order to prevent spontaneous hydrobromination. The resulting solution of the reactants was then quickly cooled to 77 K.

Radiolysis of the AC + HBr system by ^{60}Co γ-rays at 77 K leads to stabilization of active centres in the matrix, which initiates an effective chain reaction of hydrobromination on sample heating. This reaction takes place as the molecular mobility increases on heating to give system devitrification in the temperature range 87–95 K. The conversion degree depends on the pre-irradiation dose. Thus an increase in the dose from 1.5 to 20 kGy causes an increase from 12 to 25% in the conversion degree.

3.6. *Conclusion*

It should be mentioned that the method of carrying out a chemical reaction during matrix devitrification allows us to study actively the conversion of reactants at temperatures that are much lower than their melting point. In fact, in a crystal lattice, the chain reaction process is hindered owing to the low translation mobility of the reactants and the necessity to destroy the lattice itself. At the same time, selection of an appropriate vitrifying matrix makes it possible to carry out a chain reaction at quite low temperatures (much lower than the melting points of their crystals). The chemical process carried out at the lowest possible temperatures is of exceptional interest as there is a certain choice between all possible reaction paths with a temperature decrease. At low temperatures, only the path having the lowest activation energy will 'survive'.

Thus a decrease in the reaction temperature should result in a high selectivity of the process. Also, with a temperature decrease, the entropy factors that are so important for the thermodynamics of chemical reactions should here play increasingly insignificant roles; hence the equilibrium of all conversions should shift towards exothermic reactions, even those where high-order systems are formed.

4. Autowave regimes of cryochemical chain reactions

We have discovered a new phenomenon (autowave self-propagation of the cryochemical chain reaction) on investigating chemical reactions near absolute zero of temperature. On local brittle fracture of a sufficiently long sample of reactants, a chemical reaction starts on a newly formed surface. The temperature or density gradients arising during the reaction lead to further layer-by-layer dispersion of the solid sample. Because of this positive feedback an autowave of chemical conversion

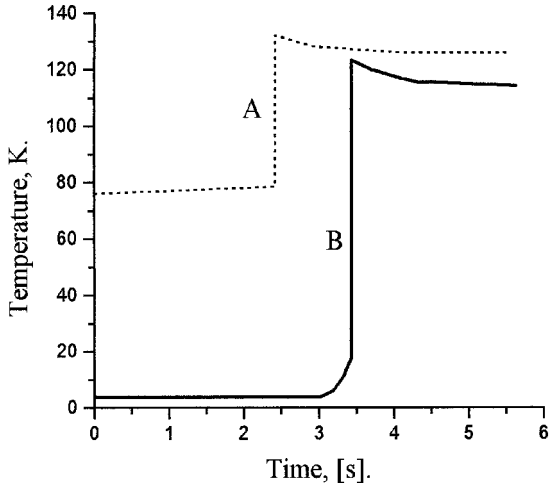

Figure 1. Temporal display of typical temperature profiles of the wave reaction $C_4H_9Cl + Cl_2$: curve A, sample immersed in liquid nitrogen (rate of wave propagation, 20 mm s^{-1}; pre-irradiation dose, 27 kGy); curve B, sample immersed in liquid helium (rate of wave propagation, 10 mm s^{-1}; pre-irradiation dose, 27 kGy).

spreads over the sample. The study has led to the discovery of highly active autowave regimes of low-temperature solid-state conversion, which became the subjects of the entire series of studies. The principal results of this first stage of these studies have been surveyed in previous reviews [10, 11]. Such an autowave regime is observed for a whole series of reactions (hydrocarbon chlorination, olefin hydrobromination, polymerization and copolymerization) at 4–77 K.

In the first experiments [66], it proved possible to initiate the spontaneous propagation of the reaction wave by means of a local perturbation. The characteristic results obtained in experiments with a cylindrical specimen of a frozen mixture of reactants (0.5–1.0 cm in diameter and 5–20 cm long) are presented below. Since the reaction was accompanied by a change in the colour of the sample, the velocity of the front was measured successfully using photography techniques. The photographs show clearly how the front, propagating parallel to itself along the axis of the cell at a constant rate of 1–2 cm s^{-1}, is formed on local mechanical breakdown.

To study the wave-front structure (its temperature profile), the autowave process was recorded thermographically in a series of experiments. The propagation velocity was measured by the time required for the wave to travel a distance (3–5 cm) between two thermocouples. The characteristic profile of the travelling temperature waves for the sample immersed in liquid nitrogen or liquid helium is presented in figure 1.

4.1. *Theory of autowave processes in solid-phase cryochemical reactions*

The model considered [67] was constructed using the following assumptions. It is assumed that the specimen is infinite in size and no account is taken of the heat exchange with the surrounding medium, that is it is assumed that the characteristic time for the evolution of the heat of reaction is much shorter than the characteristic time for the removal of heat. These conditions constitute the basis for the analysis within the framework of a one-dimensional model. According to the hypothesis, the initiation of the reaction in the given section of the specimen occurs when the stress exceeding the tensile strength of the solid matrix is generated. Since one is dealing with

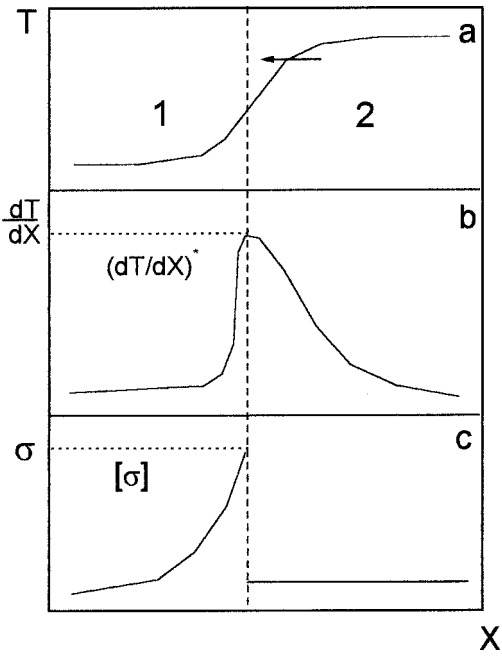

Figure 2. Characteristic forms of (*a*) the temperature profile, (*b*) the temperature gradient and (*c*) the stress field in the running wave front: (1), the zone of the specimen not involved in the reaction; (2), the zone of the specimens dispersed as a result of the reaction.

thermal stresses, and the region of elastic deformation and brittle fracture is considered, it follows that, in the given physical model, the stresses can be replaced by temperature gradients if there is an unambiguous correspondence between them (figure 2). Such a change in the variables greatly simplifies the model and makes it possible to exclude from consideration mechanical equations and to reduce the analysis to only one heat balance equation in which, instead of the limiting brittle breakdown stress, a critical value of the temperature gradient is introduced as the parameter.

Taking into account the assumptions made, the equation describing the autowave process assumes at first sight a form analogous to the fundamental equation of the theory of combustion [68]:

$$\lambda \frac{\mathrm{d}^2 T}{\mathrm{d}x^2} - U\rho c \frac{\mathrm{d}T}{\mathrm{d}x} + Q = 0, \tag{1}$$

where T is the temperature, x is the coordinate, λ is the thermal conductivity, c and ρ are the heat capacity and density respectively of the solid mixture of reactants, Q is the rate of reaction heat release and U is the rate of propagation of the thermal wave front.

However, the fundamental difference between the autowave and combustion process is that, in the former case, Q is the function of the temperature gradient but not the temperature itself. Let Q change jumpwise from 0 to Q^* at $\mathrm{d}T/\mathrm{d}x = (\mathrm{d}T/\mathrm{d}x)^*$, and let it retain this value for a certain time interval τ. This implies physically that the heat release in the reaction is switched on only in response to the brittle fracture of the sample produced by thermal stresses equal to the ultimate strength of the material. The employment of the reaction time τ as the parameter reflects that part of the hypothesis according to which the time of chemical activity during the formation of a crack is

limited by the deactivation process (for instance, by recombination of active species of fracture surfaces). In terms of the stationary model (1) considered here, the parameter τ contains information about the reaction zone (the dispersion zone) at the propagating front, whose size is equal to $U\tau$. At each point within this zone, the reaction proceeds at a rate Q^* and, outside it, $Q = 0$.

The boundary conditions can be written as

$$T|_{x=-\infty} = T_0, \quad T|_{x=+\infty} = T_0 + \frac{Q\tau}{c\rho} \equiv T_m,$$

where T_0 is the initial temperature of the sample and T_m is the maximum temperature of its adiabatic heating due to the reaction heat. The model is considered quasihomogeneous, that is it is postulated that the characteristic size of the grain formed in the dispersion zone is much less than the width of the temperature wave front.

Equation (1) with the heat source as a function of the type indicated has a solution in the form of a travelling wave. The principal attention will be paid to analysis of the dependence of the wave propagation rate on the parameters. This dependence assumes the following form:

$$g(u) \equiv [1 - \exp(-u^2)]u^{-1} = G. \tag{2}$$

Here $u = U(\tau/a)^{0.5}$ is the dimensionless velocity of a propagation wave (the parameter to be determined), $G = (dT/dx)^* a^{0.5}/(T_m - T_0)$ is the dimensionless critical temperature gradient, and $a = \lambda/c\rho$ is the coefficient of thermal conductivity.

As seen from figure 3, the autowave solution of equation (2) exists only for $G < G_0 \approx 0.64$. Physically, this implies that, in the system described by this model, the autowave mode of the reaction propagation over a solid reactant mixture become impossible for a definite increase in the strength of the sample, a decrease in the thermal effect and reaction rate, and an increase in the thermal conductivity.

An important feature of equation (2) is the non-uniqueness of its solution. In the region $G < G_0$, two values of the stationary velocity of the wave propagation correspond to the same value of G. Let us compare the characteristics of two autowave regimes. For simplicity, we shall consider the range $G \ll G_0$, in which equation (2) is soluble for U. The expression for U, corresponding to the regime with a low velocity (the 'slow' wave regime), has the form

$$U = \frac{a(dT/dx)^*}{T_m - T_0} \quad \text{or} \quad U = \frac{a(dT/dx)^*}{Q\tau/c\rho}, \tag{3}$$

while the expression corresponding to a high velocity (the 'fast' wave regime) is

$$U = \frac{(T_m - T_0)}{(dT/dx)^* \tau} \quad \text{or} \quad U = \frac{(Q^*/c\rho)}{a(dT/dx)^*}. \tag{4}$$

When the process takes place in the slow wave regime, it is possible to see features that reflect the similarity of this process, despite the differences in its physical nature. The wave velocity shows the same dependence on thermal conductivity as in flame propagation. Analogously to combustion, the reaction zone is near the maximum temperature T_{max} (it is near T_{max} that the critical gradient $(dT/dx)^*$ switching on the reaction is realized), whereas the greater part of the front temperature profile corresponds to inert heating of the sample (the 'Michelson zone' in combustion theory).

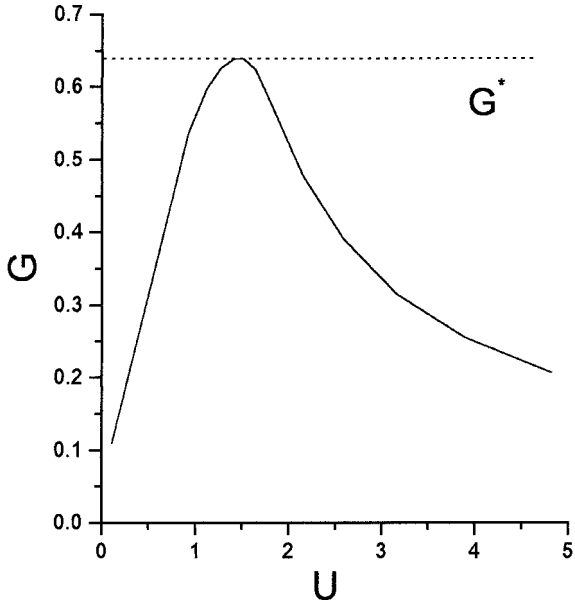

Figure 3. Dependence of the critical temperature gradient on the rate of the reaction wave propagation.

The characteristics of the process in the fast wave regime are significantly different. The most conspicuous feature of equations (4) is that the velocity does not depend on the thermal conductivity. This result, unexpected for a problem with conductive heat transfer, is connected with the peculiarities of the front structure. The temperature profile of the wave front is considerably steeper than that of the slower wave, and the reaction onset coordinate is in the front part of the wave, near T_0. It is this that explains the Q independence of the wave process, because the temperature gradients are high, approaching a critical value in the unheated part of the front. These considerations also explain the different effects of the critical temperature gradient on the two modes of the autowave process; with strengthening of the reacting sample (with increase in $(dT/dx)^*$) the velocity of the faster wave decreases and that of the slower wave increases.

The problem of stability of the two modes of steady-state propagation of the temperature wave over the sample needs separate study. From qualitative considerations it follows that the faster process is less sensitive to disturbances (both mechanical and thermal) than the slower process. Evidently, in the case of slow motion, any kind of inhomogeneity in the sample (e.g. a local reduction in the strength, leading to a decrease in $(dT/dx)^*$) may cause a displacement of the reaction onset coordinate to the front part of the wave front and thereby induce a spontaneous transformation of the slower wave into the faster wave.

Let us consider the experimental data of the previous section from the standpoint of the theoretical results presented here. The faster wave regime is closer to the experimental conditions in two respects. The first concerns the initial conditions, that is the mode initiation (ignition) of the reaction. To initiate the slower wave, the heating of a local area of the solid sample must proceed at a rate such that the time of this process is comparable with the characteristic time of thermal relaxation of the system. Indeed, it is this mode of heating that produces a temperature profile of the slower

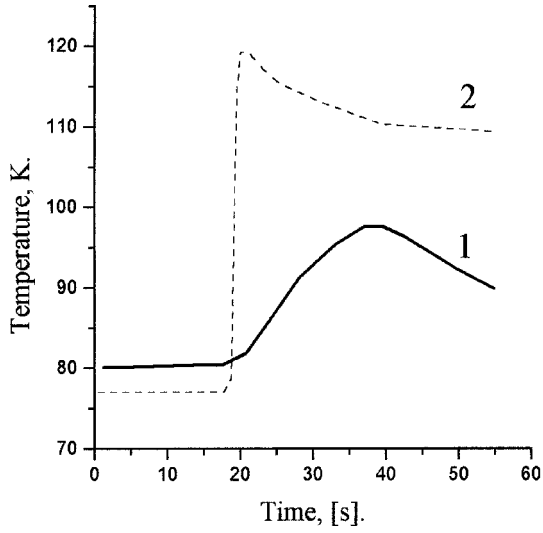

Figure 4. Time scan of the temperature profiles of the $C_4H_9Cl + Cl_2$ reaction of wave propagation on slow (curve 1) and rapid (curve 2) heating. For curve 1, $U = 1$ mm s^{-1} and, for curve 2, $U = 12$ mm s^{-1}.

wave in which the critical gradient approaches the maximum temperature. The faster wave is initiated at a high rate of heating that triggers at the initial instant of the reaction heat release in the unheated zone of the sample as a result of its dispersion. These conditions of wave initiation were realized in the first stage of the experimental study.

The second is in the structure of a travelling wave. As indicated above, the reaction zone of the faster wave front starts at temperatures close to the initial temperature. This peculiarity was revealed in the experiments carried out in liquid helium or nitrogen.

Having obtained some qualitative agreement, we shall try to make a quantitative comparison as well. To calculate the wave velocity from equations (4), we need numerical data on the temperature difference in the wave front, critical gradient and reaction duration. The values for these parameters were obtained in the experiments on the reaction dynamics and travelling waves in the butyl chloride + Cl_2 system. In particular, in liquid nitrogen we have the following values: $T_m - T_0 = 60$ K, $\tau \approx 0.1$ s and $(dT/dx)^* \approx 300$ K cm^{-1}. The calculated value $U \approx 2$ cm s^{-1} is very close to the experimental value.

To test the fit of the theoretical mechanism to the experimentally observed phenomenon, it seemed principally important to try to realize experimentally the second mode of the autowave process. Its initiation was performed, according to the theory, not by pulse heating but with the help of a heater whose temperature could be raised slowly.

In special experiments, the specimen was placed in a cryostat in boiling nitrogen vapour. Under such conditions, it is possible to observe, together with the fast wave (whose velocity did not differ from that described previously), also the slow wave (figure 4). Evidently the velocity of the slow wave is approximately an order of magnitude less than that of the fast wave, which agrees with the value calculated from equations (3) and (4).

The realization of the slower wave involved certain difficulties. Also it could not be

initiated in every experiment. There were cases when the well developed slower wave transformed into the faster wave during its propagation, so that the first thermocouple in its path recorded a front profile similar to that of the slower wave, and the second a profile similar to the faster wave. The higher sensitivity of the slower propagation mode to various disturbances has already been noted in the theoretical treatment of the autowave process.

4.2. *Autowave reactions under the conditions of uniform compression and the role of mechanical stress dynamics*

It follows from the above analysis that the effect of various factors on the strength characteristics of a solid mixture of reactants can serve to examine the ideas being developed. For this purpose, studies were made of the influence of a high pressure on the dynamic characteristics of autowave [69] and of the role of the rate of application of a stress and of the regimes in the cracking of the specimen on the excitation of the reaction by a mechanical influence [70].

In conformity with the theoretical prediction [67], an increase in the pressure applied to the specimen reduced the velocity of the reaction wave front. The decrease in velocity at a pressure of 6×10^8 Pa proved to be very considerable, approximately a factor of 2.5–3 compared with the rate of the process in the uncompressed specimen. Thus, the achievement by the matrix of a more homogeneous and ordered structure due to the compression, together with its simultaneous strengthening and the impeded fracture formation, slows down the propagation of a travelling dispersion–conversion wave. This can be naturally connected with the growth of the critical value of the temperature gradient $(dT/dx)^*$, causing brittle fracture of the sample.

The wave structure also undergoes the following typical changes, in complete agreement with the theoretical results: the front decreases with increasing pressure; the maximum gradient of the temperature profile is displaced from the front part of the wave front to the coordinate of maximum heating; in the low-temperature zone there appear 'tails' of inert heating, which become pronounced on loading. In other words, the strengthening of a solid mixture of reactants is accompanied by the development in the front structure of the slower wave.

4.3. *Autowave in polymerization*

Studies have demonstrated the wide occurrence of the autowave phenomenon in cryochemical reactions of solids with the identity of their physical mechanisms in a wide range of chemical systems. This justifies the hypothesis that autowave reaction regimes can prove useful for the creation of new non-traditional chemical technologies. In the autowave processes described above, the principal technological problems (activation of the chemical system, supplies of energy, and mixing of the reactants) are solved by combined procedures involving the use of the energy of the chemical reaction. The high rates of the chemical reaction occurring at low temperatures in the autowave regime are also extremely attractive. All this has stimulated the search for new objects to study.

The principal ideas concerning the mechanochemical feedback in an autowave process were confirmed in the study of this system. An autowave polymerization regime occurred in polycrystalline acetaldehyde already at 4.2–77 K and its principal characteristics were investigated [71]. The polymerization wave in crystalline acetaldehyde was observed in bulk (cylindrical) and thin-film specimens at 77 or 4.2 K. The wave was excited in response to the local brittle fracture of frozen acetaldehyde.

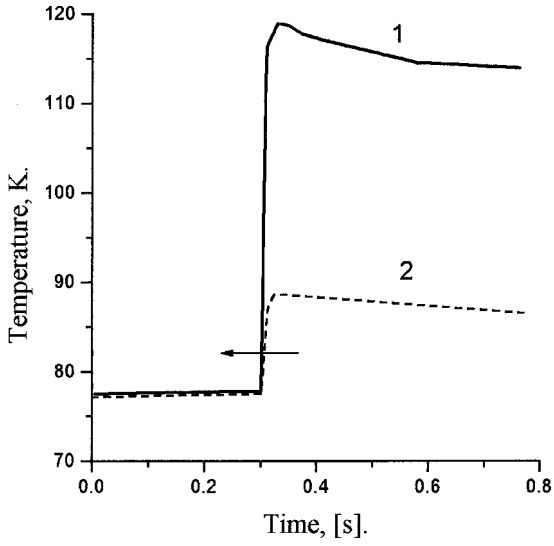

Figure 5. Temperature profiles of the reaction wave in the radiolysed (curve 1) and photolysed (curve 2) system $C_4H_9Cl + Cl_2$. The initial concentration of alkyl radicals in both cases is 2×10^{18} l g^{-1}. The rate of wave propagation is 10 mm s^{-1} for curve 1 and 400 mm s^{-1} for curve 2.

When the autowave passed through the specimen in the helium bath, the maximum temperature in the front did not exceed about 130 K, that is it was significantly lower than the melting point of the monomer (150 K). Consequently this system provides an example of an autowave process occurring exclusively in the solid phase. According to the ideas being developed, the chemical reaction front consists of a mechanical dispersion zone moving in the solid reactant. Examination of the photographs recording the passage of the wave established that behind the front the initially opaque polycrystalline specimen is fully clarified. It could be assumed that this clarification is associated with the amorphization of the specimen.

4.4. *Autowave in photoactivated systems*

Here we consider the experiments on the local mechanical initiation of a reaction in photoactivated solid matrices [72]. It has been found that preliminary treatment of previously investigated solid systems, for example $C_4H_9Cl + Cl_2$, at 77 K not by γ-radiation but by light also leads to the accumulation in the matrix of potential energy, which can be used for the subsequent initiation of a specific chemical reaction with the aid of local mechanical breakdown. Under these conditions, the process occurs, as in the case of γ-irradiation, in the form of a layer-by-layer dispersion running wave accompanied by a chemical reaction. Furthermore, in the first experiments designed to investigate autowave reaction regimes in photolysed matrices, new features were discovered besides the usual features characteristic of self-propagation reactions in a solid at low temperatures.

We shall compare the principal characteristics of reaction autowaves in radiolysed and photolysed $C_4H_9Cl + Cl_2$ systems at 77 K (figure 5). In the front of a wave propagating in a photolysed specimen, there is no pre-explosive heat exchange, as in the radiolysed system. However, the other characteristics of the wave processes differ appreciably. Indeed the propagation rate of the front in the photolysed system is

significantly higher (about 400 mm s^{-1}) than in a radiolysed system (about 10 mm s^{-1}) for identical concentrations of stabilized alkyl radicals.

The temperature profiles of the front also differ greatly; the maximum temperature in the radiolysed system is 121 K, while in the photolysed system it is only 83 K, that is in the latter case the superheating in the reaction zone relative to the thermostat reaches only about 6 K. These differences are probably associated with the difference between the mechanisms of the chemical reactions occurring on mechanical breakdown. For the same initial concentrations of the alkyl radicals, the initial reaction rate in the radiolysed system is lower than in the photolysed system, because some of the chlorine atoms propagating the chain are captured by chlorine ions that are not formed on photolysis.

The problem of the vibrational instability in the movement of the cryoreaction front, demonstrated by the pulsating character of the cryowave in the methylcyclohexane–chlorine system, has been formulated [73]. The hypothetical mechanism of this phenomenon is based on the fact that in the radiolysed system the zone corresponding to dispersion induced by the chemical reaction moves ahead abruptly (at rates of the order of the velocity of sound) to a depth comparable with the characteristic fragmentation grain size. The chemical reaction begins in this disrupted layer and a new jump of the reaction zone in space occurs only after a critical density or temperature gradient is attained. Since the rate of the chemical reaction in the breakdown zone of the photolysed system is higher, the necessary conditions for the next jump of the reaction zone are attained faster than in the radiolysed system, which increases the average velocity of the wave.

4.5. *Cryo-autowaves of the detonation type*

We observed similar phenomena in experiments with unirradiated thin-film ethylene + chlorine, propene + chlorine and vinyl chloride + chlorine cocondensates [74]. It was possible to establish that the chlorination of these hydrocarbons at 77 K takes place not in the form of a homogeneous explosion but as an autowave regime, and the film is pricked and is characterized by extremely intense dispersion in the front of the self-propagating reaction, which is indicated, in particular, by the 'recoil' of finely dispersed fragments of the reacting matrix accompanying the wave. The second factor as well as the high velocity of the front (tens of centimetres and even metres per second) give grounds for agreement with Barelko *et al.* [11], who believed that yet another variety of low-temperature wave, mechanochemical in nature and close in its essential physical features to detonation phenomena (admittedly with features of degeneracy, namely pre-sonic velocities), may exist in a solid.

This problem is complex and requires development of fundamentally new theoretical and experimental approaches to elucidate the mechanisms of the chemical reaction energy transfer in low-temperature detonation processes in solid systems. Here one is dealing not with the usual mechanism of the detonation wave excitation, known in the classical theory of explosion, but with an unusual type of detonation which may be called gas-free detonation.

4.6. *Conclusion*

Now, it is important to define the place occupied by the above phenomena in the general series of different self-propagating chemical processes. For this purpose, we shall attempt to classify the chemical systems characterized by autowave phenomena. Without going into detail, we shall differentiate the phenomenological features of two

large groups to which virtually any of the systems of the kind known at present can be assigned: firstly processes of the combustion type (the factor determining the existence of the running wave regime in this case is thermal nonlinearity); secondly processes of the branched-chain type (the so-called 'chain combustion' associated with kinetic nonlinearity of an autocatalytic character). Evidently the self-activation mechanism of a frozen reactive system, which determines the characteristic feature of the wave processes, is essentially close to the branched-chain mechanism.

The concept of the branched-chain mechanism in solid-state chemistry is itself not new and has been discussed in the literature for many decades [75, 76]. It is constructed on the basis of the claim that the active centres ('nuclei') of the reaction are all kinds of defect distributed in the solid matrix of the reactants and progressively multiplying on it when acted upon by the effects induced in the solid by the reaction itself. The operation of this mechanism has been examined in the greatest detail and most convincingly in a large series of investigations [77–81] of the thermal decomposition of ammonium perchlorate at temperatures of about 500 K.

These studies, in which the changes in the structure of a decomposing crystalline specimen were observed, established firstly that the reaction of the solid reactant takes place within the framework of the strong influence on the process of mechanical stresses induced by the decomposition reaction and consists of stages involving the formation and growth of the reaction 'nuclei', their multiplication, an increase in their density and their coalescence and secondly that, on coalescence of the separately developing reaction zones, a single reaction front may be formed and can move within the specimen in the form of a cloud of multiplying nuclei at low but quite definite velocities (about 10^{-4} mm s^{-1}).

Critical phenomena, which are known to constitute a necessary feature of branched-chain and autowave processes, were not considered in these studies. This is most probably due to the retention by the thermal mechanism of the leading role in the perchlorate decomposition reaction. This is in fact indicated by the pronounced exponential dependence of the overall rate of salt decomposition (as well as of the velocity of the front) on temperature; on cooling, the reaction rapidly slows and is almost completed already at 460 K. One should add that the perchlorate decomposition reaction is not strictly a solid-phase reaction, because it is accompanied by a change in the phase state.

Several years ago, the concent examined above was extended to low-temperature solid-state chemistry. Benderskii *et al.* [82] used the idea of self-activation of the matrix due to the feedback between the chemical reaction and the stressed state of the frozen specimen comprising the reactants to explain and describe the so-called 'explosion on cooling', which they observed in the photolysed methylcyclopentane + Cl_2 system. The model proposed [82–84] is unfortunately not entirely concrete, because it operates with an abstract quantity called by Benderskii *et al.* the 'excess free energy of internal stresses'. Furthermore, to achieve the feedback, these researchers had to introduce into the model the thermal balance equation, although their claims are based on non-thermal ideas about the mechanism of the self-activation of reactants at low temperatures. Nevertheless, the essential features of their ideas [82–84] can be formulated by the following phenomenological postulate: the mechanical energy accumulating in the matrix promotes directly an acceleration of the chemical solid-phase reaction by a subsequent reduction in its activation barrier. In other words, the proposed model of low-temperature reactions in a solid is constructed wholly within the framework of the classical Arrhenius kinetics supplemented merely by certain

elements of the kinetic theory of mechanical strength [85]. The question of the existence of autowave remains almost fully outside these investigations.

We should like to draw attention to an important methodological factor that might have escaped the attention of Benderskii *et al*. [82–84]. This concerns the influence of the material of the cells on the conditions of initiation of the photochemical reaction. When experiments are carried out in γ-irradiated or photolysed systems, cooling of the specimen can, as already stated above, induce a rapid reaction. However, a decisive factor is not cooling but the rate of temperature decrease. By reducing the rate of cooling, it is easy to maintain the specimen in a fully inert state down to 4.2 K. However, this is characteristic only of Pyrex bulbs. Another picture is observed when quartz bulbs are used. The strict reproducibility of 'explosion on cooling' [82–84] might have been associated with the exclusive use of quartz cells in the experiments. The coefficient of the thermal deformation of this material differs greatly (in contrast with that of ordinary glasses) from that of the reactants, and the result is that the inevitable peeling of the substance from the walls of the bulb on cooling (i.e. fracture) induces the 'explosion' described in [82–84].

The ideas that we have developed concerning the nature of autowave highly intense regimes in a cryochemical reaction are based on a mechanism that can be called an 'energy chain'. It follows from the data presented in this review that this analogy is entirely justified because the proposed mechanism involves a chain of stages, closed by positive feedback and accompanied by energy transformations of the chemical conversion in time and space. Indeed, it is suggested that, during the reaction, part of the energy is accumulated in the solid matrix in the form of elastic deformation, that is the unreacted part of the specimen passes in this stage to a mechanically non-equilibrium and, in a certain sense, 'excited' state; the potential energy of this metastable state is then transformed into chemical energy. However, the transformation is not direct and occurs only through the brittle breakdown stage in which conditions are created for the chemical reaction occurring on freshly cleaved surfaces or near them where the energy has been concentrated. This mechanism determines the self-maintaining regime in the reaction of a solid specimen excited by layer-by-layer autodispersion. Ideas postulating the branched-chain character of the process are visualized by the pattern of the continually branching and migrating network of cracks in the reacting matrix.

The developed postulates must also account for the processes involving the 'cold' evolution of matter in the Universe, that is the formation of increasingly complicated molecules of elements under the conditions of interstellar dust.

Beginning from its birth in the 'Big Bang' during physical evolution the substance of the Universe could pass through a series of cycles of strong heating. The end of any of those cycles might be the starting point of further chemical evolution of the substance in the Universe. It is natural to think that, during the cycle of heating, the substance existed and evolved only in the form of chemical elements. Further cosmic processes led to its approximately fast cooling to temperatures near absolute zero. The formation of molecules from elements and their further complication could take place only during such cooling. Molecular gases (hydrogen, oxygen, nitrogen and carbon oxide) were formed. If these gases were frozen out on the grains of interstellar dust or on cold planets, then, based on classical notions, their further existence became very problematical, even in spite of the cosmic time scale. At the same time, a number of external planets and their satellites had oceans of ammonia and methane. There was also a sufficient amount of these gases and water in interstellar space.

One can imagine the process of formation of compounds, such as ammonia and methane, out of a frozen mixture of elements from the surface of cold planets and their satellites in the following way. Those cosmic objects had sharp daily changes in temperatures. The thermal stresses arising in the solid crust of the planet were an instrument of its continuous destruction. Such multifold brittle fracture of a frozen mixture of elements that were previously made active by solar radiation might result in chemical binding of elements. The same might be true also for interstellar clouds, gigantic suspensions of dust grains in the gas. The dust grains are assumed to possess nuclei of silica or graphite surrounded by a coat of 'dirty ice', a frozen mixture of gases.

The next stage of chemical evolution, when solid ammonia and hydrocarbons that were continuously dispersed in a 'solar mill' might transform into amines, is also highly probable. The formation of long polymeric chains at brittle fracture under the conditions of cosmic cold is believed to be experimentally proved from the examples of the polymerization of formaldehyde and acetaldehyde.

The next natural stage necessary to confirm the above hypothesis should be direct experimental evidence of the series of cryosyntheses described here. The nitrogen–hydrogen system is thought to be the most interesting. Dispersion and autodispersion of a radiolysed mixture of solid hydrogen and nitrogen may be thought to lead to the formation of hydrazine or ammonia. The carbon–hydrogen system may prove to be no less interesting, there being two possible variants: dispersion of a solid mixture and dispersion of carbon in liquid hydrogen. Research into these fields is thought to have more prospects as it may lead to creation of new unconventional technologies.

The processes involving the transition of a solid from a metastable amorphous state to a polycrystalline state, which have been vigorously investigated (see [56] and references therein), are autowave in character and outwardly resemble the solid-phase cryochemical reactions considered in this section. In this class of processes, one cannot rule out the operation of the same autodispersion mechanism, facilitating the phase transformation as a result of its transfer from the bulk phase to the fracture surface. Indeed, both classes of processes resemble one another concerning their essential physical features and are associated with the rearrangement of the solid matrix. Both are exothermic and differ only in the magnitude of the thermal effect. Furthermore, one should add that the cracking and dispersion of the specimens, which can be observed even with the naked eye, are extremely typical of the wave processes involving the decomposition of amorphous states.

One more possible application of the ideas about self-maintaining phase transitions in a solid, formulated in a brief communication by American geophysicists, is extremely interesting [86]. They put forward a hypothesis according to which the phase transformation in terrestrial rocks as a result of the operation in them of an autocatalytic self-disruption mechanisms are the main cause of earthquakes and other catastrophic geotectonic processes.

In concluding the review of studies on the phenomena involving the running waves of cryochemical reaction in a solid and of the analysis of the mechanisms controlling these processes, we may note that the studies that have been carried out are mainly phenomenological in character. Naturally, the next task is the solution of a wide range of fundamentally important problems associated with the elementary stages of the process. The main problems are the elucidation of the nature of active states arising on the cleavage planes, their lifetimes, the establishment of the mechanism of intensification of transport processes on fresh fracture surfaces, the search for electrical

signals associated with emission of charged particles during the cracking process, and the search for signals of the type of triboluminescence arising from the front of the dispersion (chemical reaction) running wave.

5. Rate oscillations of the solid-state chemical reaction

5.1. *Introduction*

The oscillation rate of chemical conversion, unusual for traditional concepts, has attracted considerable attention [87–92]. The discovery itself and the experimental confirmation of the variations in the chemical reaction rate have a long and quite an instructive history. Modern interest in this field was initiated by Belousov's discovery of the fluctuations of concentrations of oxidized and reduced cerium forms in the oxidation of citric acid with cerium ions, catalysed bromate. Later this reaction was studied in detail by Zhabotinskii; hence this reaction is called the Belousov–Zhabotinskii reaction.

This section of the review reports auto-oscillation regimes of chain low-temperature radiation-initiated chemical reactions having a thermokinetical character [93–98]. For reactions proceeding under isothermic conditions, the reaction mechanism reaction necessary for the rate variation to arise is created only by chemical autocatalysis. For chain exothermic reactions the released reaction heat can serve under certain conditions as the feedback connection. The heat release can increase the ambient temperature and hence also the chemical conversion rate. Therefore, heat release can perform a function analogous to autocatalysis. The thermokinetic models of auto-oscillations of chemical reaction rate were studied by Sal'nikov [99, 100]. A detailed description of such regimes of reactions can be found in the published monographs in [87, 91, 92].

Cryochemical conversions offer a fertile field for thermokinetic oscillations; the defectivity of solid matrices, because of their low heat capacities, account for the temperature field irregularity. Below we shall discuss many studies on the auto-oscillation regime of cryochemical conversions in glassy and crystalline matrices.

5.2. *Auto-oscillatory regime for cryochemical conversion during irradiation*

We first came across auto-oscillations of the cryochemical conversion rate when studying the radiation hydrobromination of ethylene [93]. The auto-oscillations of the cryochemical conversion rate were observed at a thermostat temperature of 85 K after switching on γ-radiation (figure 6). These rate auto-oscillations die out with time as reactants are consumed. The total extent of the reactant conversion for the experiment represented in figure 6(*a*) was about 40%. On repeatedly switching on the γ-radiation, the presence of some characteristic conditions necessary for such an oscillatory regime of the reaction to occur is required:

(1) an auto-oscillatory regime is observed only at thermostat temperatures above 75 K;
(2) oscillations of the radiation hydrobromination rates arise only when the dose rate of the initiating radiation exceeds 0.2 Gy s^{-1} (higher than the certain rate of heat release at the expense of the reaction).

Figure 6(*b*) shows an experiment carried out under the same conditions as that in figure 6(*a*) but with the dose rate of γ-radiation decreased to 4×10^{-4} Gy s^{-1}. Auto-oscillations of the hydrobromination rate are no longer seen to arise.

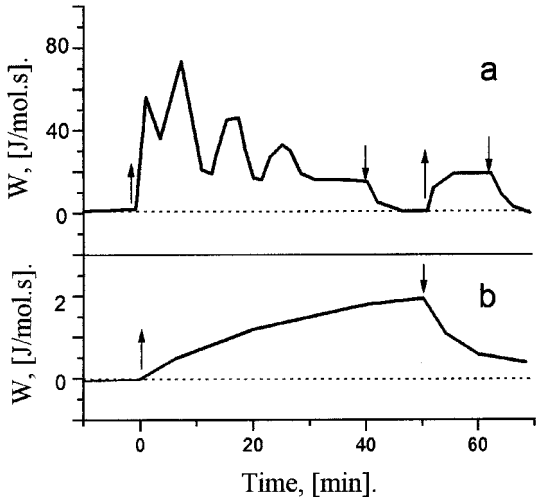

Figure 6. Rate variations of radiation-induced ethylene hydrobromination at a thermostat temperature of 85 K: (*a*) dose rate of 0.3 Gy s^{-1}; (*b*) dose rate of 4×10^{-4} Gy s^{-1}. The moments of switching the γ-radiation on and off are shown by arrows.

Since the moment of switching on the γ-radiation, the reaction (heat release velocity) increases in time owing to an increase in the concentration of active centres. If the heat removal is not enough, some overheating of a sample relative to a thermostat can occur. The value of overheating increases with an increase in the reaction rate. However, the temperature rise leads to an increased rate of disintegration of active centres, thus decreasing the total concentration of active centres. Such a decrease results in a fall in the process rate and, as a consequence, to a decreased value of sample overheating relative to the thermostat. The decreased value of overheating returns the system again to the temperature region where accumulation of the active centres up to a higher concentration may occur, this again leading to an increased reaction rate. Therefore, the auto-oscillation of the reaction rate discovered in the radiation-induced solid phase hydrobromination of ethylene has a thermokinetic character. It should be noted that the auto-oscillations in the case of a solid-phase chain reaction are experimentally observed for the first time.

It is obvious that the auto-oscillatory regime is possible only with intensive heat release. The use of low initiation rates (low dose rates) leads to low values of sample overheating and, as is clear from our experiment, the auto-oscillatory regime becomes degenerate. Auto-oscillations in the HBr + ethylene system would probably start at temperatures above 70 K as in this range there is a sharp increase in the total reaction rate with a temperature rise (activation energy, about 17 kJ mol^{-1}). At lower temperatures (70 K or less) the hydrobromination rate depends weakly on temperature (activation energy, 750 kJ mol^{-1} or less) and no auto-oscillations in this temperature region are observed.

To test the above idea, experiments have been carried out under the conditions of heat removal from a sample especially made badly. With an increase in the dimensions of the initial sample, some non-uniformity of the temperature field is observed, and this leads to auto-oscillations. The development of the latter can take place both in time and in space.

Let us examine a mathematical model of the auto-oscillatory regime of radiation-

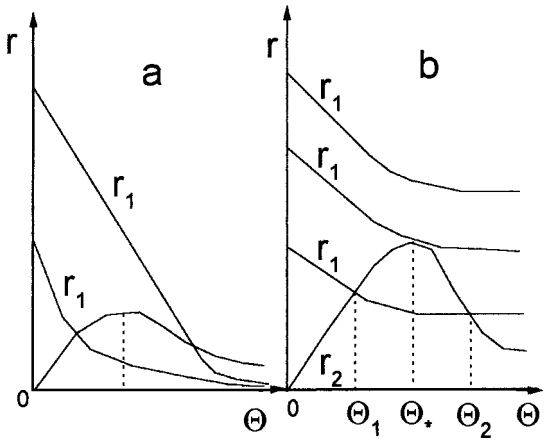

Figure 7. For explanation see text.

induced solid-phase hydrobromination of ethylene. It is known that the radiation-induced hydrobromination of ethylene involves the following steps:

(1) initiation of chain: $HBr \rightarrow H + Br$ (γ-ray);
(2) chain propagation: $Br + C_2H_4 \rightarrow C_2H_4Br$,
$C_2H_4Br + HBr \rightarrow C_2H_5Br + Br$;
(3) chain termination: $R \rightarrow$ monomolecular,
$R + R \rightarrow$ bimolecular.

Here R is Br or C_2H_4Br. In the solid state, this reaction takes place through the equimolar complex $C_2H_4 \cdot HBr$. The non-isothermal occurrence of the reaction according to this scheme is described by the following differential equations: for the consumption of the starting reactant (complex $C_2H_4 \cdot HBr$) by

$$\dot{M} = -\kappa(T) RM, \tag{5}$$

for the balance for active centres by

$$\dot{R} = gJ - k_1(T) R - k_2(T) R^2 \tag{6}$$

and for the heat balance by

$$c\rho\dot{T} = Qk(T) RM - \alpha\frac{S}{V}(T - T_0). \tag{7}$$

These equations must be solved for the following initial data:

$$t = 0, \quad M = M_0, \quad R = 0, \quad T = T_0. \tag{8}$$

Here M, R and T are differentials with respect to t, T and T_0 are the temperatures of the thermostat and the reactor respectively, Q is the heat of the reaction, α is the heat transfer coefficient to the walls, S/V is the geometric factor expressing the ratio of the surface area of the reactor to its volume, c and ρ are the heat capacity and the density respectively of the substance in the reactor (which are considered to be constant), J is the dose rate of γ-radiation, g is the radiation yield of active centres, and $\kappa(T)$, $k_1(T)$ and $k_2(T)$ are the reaction rate constants, which are assumed to be Arrhenius functions

of temperature with activation energies E, E_1 and E_2 respectively (this is true for the temperature range 50–70 K). Let us introduce the dimensionless variables

$$\tau = t\frac{\alpha}{c\rho}\frac{S}{V}, \quad m = \frac{M}{M_0}, \quad r = R\frac{\alpha}{c\rho gJ}\frac{S}{V}, \quad \Theta = \frac{E(T-T_0)}{R_0 T_0^2}, \tag{9}$$

and the dimensionless parameters (R_0 is the gas constant in the Arrhenius law)

$$\varepsilon = k(T_0)\, gJ\left(\frac{c\rho}{\alpha}\right)^2\left(\frac{V}{S}\right)^2, \quad \xi = \varepsilon M_0\frac{QE}{c\rho R_0 T_0^2}, \quad p = k_1(T_0)\frac{c\rho}{\alpha}\frac{V}{S},$$

$$q = \varepsilon\frac{k_2(T_0)}{k_2(T)}, \quad \nu = \frac{E_1}{E}, \quad \mu = \frac{E_2}{E}, \quad \beta = \frac{R_0 T_0}{E}. \tag{10}$$

In these variables, equations (5)–(7) and conditions (8) take on the more convenient forms

$$\dot{m} = \varepsilon mr\exp\left(\frac{\Theta}{1+\beta\Theta}\right), \qquad m(0) = 1, \tag{11}$$

$$\dot{r} = 1 - pr\exp\left(\frac{\nu\Theta}{1+\beta\Theta}\right) - qr^2\exp\left(\frac{\mu\Theta}{1+\beta\Theta}\right), \qquad r(0) = 1 \tag{12}$$

$$\dot{\Theta} = \xi mr\exp\left(\frac{\Theta}{1+\beta\Theta}\right), \qquad \Theta(0) = 0. \tag{13}$$

In the following, to simplify the calculation, we make use of the approximation $\beta = 0$ [3]. Let us consider the case of small values of ε (or small gJ; see equation (10)), and let us study the behaviour of r and Θ against the background of a slow evolution of m. In particular, we shall be interested in the possibility of self-oscillations in r and Θ. We note that investigation of the behaviour of the fast variables when the value of the slow variables is 'frozen' has a rigorous mathematical basis presented in [101], for the case when r and Θ (for $\tau \to \infty$) makes a transition to a stable stationary state, and in [102], when r and Θ make a transition to a stable periodic regime.

In this stage of the investigation, let us restrict ourselves to considering only monomolecular chain termination and neglecting bimolecular termination, that is let us set $q = 0$ in equation (12). This assumption is acceptable in the region $q \ll 1$ and considerably simplifies the mathematical analysis, reducing the number of parameters to three: ξ, p, ν (see equation (10)). Let us rewrite equations (12) and (13) taking into account this simplification and the abbreviation $\lambda = \xi m$ for the frozen value of m:

$$\dot{r} = 1 - pr\exp(\nu\Theta), \quad \dot{\Theta} = \lambda r\exp(\Theta) - \Theta. \tag{14}$$

The stationary points of system (14) are the points of intersection in the (r, Θ) plane for the curves:

$$r_1 = \exp(-\nu\Theta)\frac{1}{p}, \quad r_2 = \Theta\exp(-\Theta)\frac{1}{\lambda}. \tag{15}$$

When $\nu \geqslant 1$, these curves intersect at only a single point (figure 7(*a*)). When $\nu < 1$, either the curves (5) intersect at two points or there is no point of intersection (figure 7(*b*)). The condition for tangency of the curves (15) leads to the following relationship between p and λ:

$$p = p_*(\lambda) = \exp[\lambda(1-\nu)], \tag{16}$$

dividing the region where there are no stationary points $p < p_*(\lambda)$ and the region where there are two stationary points $p > p_*(\lambda)$. The intersection points Θ_1 and Θ_2 of the curves (15) are divided by their tangency point $\Theta_* = (1-\nu)^{-1}$ (figure 7(*b*)):

$$\Theta_1 < \Theta_* = (1-\nu)^{-1} < \Theta_2. \tag{17}$$

The system of equations linearized in the neighbourhood of some stationary point (Θ_0, r_0) has the form

$$\dot{u} = -\frac{u}{r_0} - \nu w, \quad \dot{v} = \frac{u\Theta_0}{r_0 + (\Theta_0 - 1)\, v}. \tag{18}$$

The determinant Δ and the trace S of the coefficient matrix for the right-hand side are expressed by the formulae

$$\Delta = \frac{1}{r_0}[1 - (1-\nu)\,\Theta_0], \quad S = \Theta_0 - 1 - \frac{1}{r_0}. \tag{19}$$

From this it is obvious that $\Delta > 0$ for $\nu \geqslant 1$, and in the case $\nu < 1$ the inequality $\Delta > 0$ is satisfied at the low-temperature stationary point $\Theta_0 = \Theta_1$ (see equation (17)). At the point Θ_2, as can be seen, $\Delta < 0$.

Thus, around the two stationary points, the high-temperature point has the character of a 'saddle point'; the low-temperature point, like the single stationary point for $\nu \geqslant 1$, has the character of a 'node' or 'focus'. From the standpoint of the possibilities for self-oscillation, it is important to determine the region of instability for the node and focus:

$$\Theta_0 > \frac{1 + r_0}{r_0}. \tag{20}$$

In the plane of the parameters p and λ (for fixed ν), the boundary r_0, Θ_0, is determined by the parametric curve:

$$p = (\Theta_0 - 1)\exp(-\nu\Theta), \quad \lambda = \Theta_0(\Theta_0 - 1)\exp(-\Theta), \quad \Theta_0 > 1 (\Theta_0 < \Theta_* \text{ when } \nu < 1). \tag{21}$$

In the (p, λ) plane of figure 8 we show schematically the dynamics of the instability region (region I) for variation in ν. For $\nu < 1$, we consider the instability region of the low-temperature stationary state. In the additional region II, there is stability. When $\nu < 1$, region III arises, a region in which there are no stationary states. The boundary of region III is defined by the straight line (16). The curvilinear boundary of region I is calculated using equation (17). The maximum value $p_{\max} = \nu^{-1}\exp[1(\nu+1)]$ is reached when $\Theta_0 = \Theta_p = 1 + \nu^{-1}$. The maximum value is $\lambda_{\max} = 0.309$. As is evident, $\lambda_{\max}$ does not depend on ν, while $p_{\max}$ increases with decrease in ν. When $\nu \geqslant 1$, curve (21) describes region I (figure 8) with a lobe shape, when Θ_0 varies from 1 to ∞. For $\nu < 1$, at the point $\Theta_0 = \Theta_*$ (see equation (17)) this curve becomes a straight line (16). In figure 8(*b*),

$$\begin{aligned} \lambda_* &= \lambda(\Theta_*) = \nu(1-\nu)^{-2}\exp[-(1-\nu)^{-1}], \\ p_* &= p(\Theta_*) = \nu(1-\nu)^{-1}\exp[-(1-\nu)^{-1}]. \end{aligned} \tag{22}$$

For a further increase in ν, the value Θ_* increases and, when $\nu = \nu_* = (5^{1/2} - 1)/2$, $\Theta_* = \Theta_p = \Theta_s = (3 + 5^{1/2})\,2 = 2.62$, $\lambda_* = \lambda_{\max}$ and $p_* = p_{\max}$ are simultaneously satisfied (see equation (22)). At this moment, region I takes on the formula of the line (figure 8), and λ_* is its maximum value; p_* still continues to increase up to $\nu = \frac{1}{2}$; for further decrease in ν, the quantity p_* decreases together with λ_* down to zero where $\nu \to 0$.

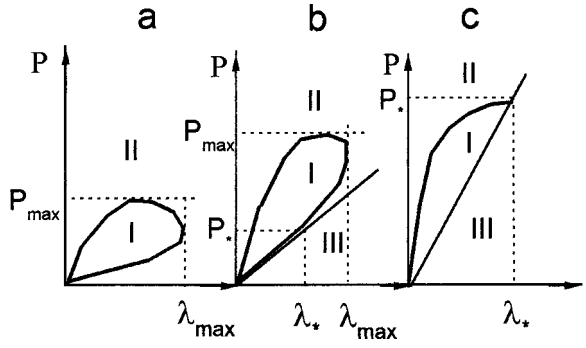

Figure 8. For explanation see text.

Together with λ_* and p_*, region I also disappears. The dynamics of the region of instability I in the parameter plane (p, λ) when the third parameter ν is decreased are shown in figure 8 (*a*) for $\nu \geqslant 1$, in figure 8 (*b*) for $\nu_* < \nu < 1$ and in figure 8 (*c*) for $\nu \leqslant \nu_*$.

In all the regions of instability for the node or focus type, system (14) has a stable limit cycle on the phase plane (r, Θ), that is, a self-oscillation solution that is periodic in time. The existence of the limit cycle is ensured by the fact that some trajectory in the system (14), which does not coincide with the stationary point, remains in the restricted part of the phase space (r, Θ) (see equation (10)). This may be most simply shown in the case of $\nu \geqslant 1$, when there is no other stationary point and the discussion and constructions in [103] (satisfied for another system of equations) remain in force. However, the restricted nature of the solution to system (14) is obvious if the exponents remain restricted ($\beta > 0$; see equations (12) and (13)). Close to the curvilinear boundary to region I (figures 8 (*b*) and (*c*)), the well known Hopf bifurcation occurs, 'soft' generation of a cycle from a focus [104]. Sinusoidal collisions of small amplitude appear with frequency (see equation (19)):

$$\omega = \Delta^{0.5} = \{(\Theta_0 - 1)[1 - (1 - \nu)]\Theta_0\}^{0.5}, \quad \Theta_0 > 1 (\Theta_0 < \Theta_* \quad \text{for } \nu < 1). \qquad (23)$$

In figure 8, we thus present a diagram for the regions of parameters corresponding to qualitatively different solutions to equations (14). In region I, as has already been noted, the solution makes a transition to the self-oscillatory regime. In region II, a stationary state is established. In region III, where system (14) does not have any stationary state, an unlimited increase in the temperature Θ occurs after a finite time (thermal explosion).

In the complete system of equations (11)–(13) (when $\beta = 0$ and $q = 0$) for rapid oscillations in r and Θ, a slow decrease in m is described by equation (11) with the right-hand side averaged over the period of the oscillations [101]. We shall not write out this equation. We shall only note that, if at the initial instant $\tau = 0$ the parameters p and $\lambda = km = m$ fall within region I, then, in proportion to the decrease in m, the point (p, λ) leaves region I. This is in agreement with the experimental observations [1], where the disappearance of self-oscillations is noted for a certain degree of conversion of the starting reactant. The mathematical model also agrees with the experimental fact that the self-oscillations are not observed for low dose rates [87]. With a decrease in gJ (see equation (10)), ε decreases and, consequently, $\lambda = \xi m$ also decreases; the point (p, λ) leaves region I. As has already been noted, upon leaving region I (figure 7) through the curvilinear section, the boundaries of the oscillations take on a sinusoidal character

and their amplitude decreases. This is also evident from the experimental curve (figure 6). It is possible to compare quantitatively the oscillation frequencies taken from the experimental curve with equation (23). It is also of interest to compare quantitatively the critical conditions for transition between regions I–III and the experimental measurements, and to use the mathematical model for solving the inverse problem of determining the model parameters by their identification with the experiment. The investigation performed shows that, for development of an oscillation reaction regime, it is sufficient to have chain termination either by only a monomolecular mechanism or by only a bimolecular mechanism.

5.3. *Post-radiation polymerization; oscillation of conversion rate*

Post-radiation polymerization taking place in a thermostat with a temperature varying linearly in a time, $T = T_0 + \Omega t$, is initiated owing to gradual liberation of the active centres with the matrix temperature rise. A certain number N_0 of active centres stabilized in a matrix is produced by a fixed γ-radiation dose. Specimens are irradiated at a sufficiently low temperature that all the active centres are stabilized and thereby a reaction during irradiation is excluded. If the chemical radiation yield of the active centres is denoted by g, then $N_0 = gD$, where D is the radiation dose.

As the temperature rises, the active centres stabilized in the matrix are liberated and initiate the reaction. We assume that the rate of active centre liberation is an Arrhenius function of temperature with an activation energy E that defines the depths of the potential wells in which the active centres are trapped during γ-irradiation. Active centres liberated owing to the temperature rise participate in the reaction and decay either owing to their spatial isolation in traps other than the radiation-induced traps (monomolecular destruction mechanism) or due to bimolecular recombination.

5.3.1. *A mathematical model of the process*

A mathematical model of the radiation-induced polymerization is suggested on the basis of the above concepts. A qualitative analysis of the model assuming a slow change in the thermostat temperature and slow consumption of both initial reactant and stabilized active centres reveals the feasibility of a self-sustaining oscillatory reaction regime, which is consistent with the experimental data on post-radiation polymerization of crystalline heptylacrylate. A method for determining the kinetic parameters from a comparison of the experimental and theoretical results obtained for the steady-state reaction regime is discussed.

5.3.1.1. *The governing equations*. Non-isothermal radiation-induced post-polymerization is described by the following differential equations: for reactant consumption by

$$\frac{\mathrm{d}M}{\mathrm{d}t} = -\,MRk(T), \tag{24}$$

for consumption of the stabilized active centres by

$$\frac{\mathrm{d}N}{\mathrm{d}t} = -\,Nk_1(T), \tag{25}$$

for the balance of active centres leading to a post-polymerization process by

$$\frac{\mathrm{d}R}{\mathrm{d}t} = Nk_1(T) - Rk_2(T) - R^2k_3(T) \tag{26}$$

and for the thermal balance by

$$c\rho\frac{\mathrm{d}T}{\mathrm{d}t} = Qk(T)\,RM - \alpha\frac{S}{V}(T - T_0 - \Omega t). \tag{27}$$

These equations are to be solved with the following initial conditions:

$$t = 0, \quad M = M_0, \quad N = N_0, \quad R = 0, \quad T = T_0. \tag{28}$$

Here T_0 is the initial thermostat temperature later on being scanned at a rate Ω, T is the reactor temperature, Q is the reaction heat, α is the coefficient of heat transfer to the walls, S/V is the geometry factor equal to the ratio of the reactor surface to its volume, c and ρ are the specific heat and density respectively of the substance in the reactor assumed to be constant, and $k(T)$, $k_1(T)$, $k_2(T)$ and $k_3(T)$ are the rate constants whose variations with temperature are governed by Arrhenius functions with activation energies E, E_1, E_2 and E_3 respectively.

It should be noted that this mathematical model also describes the process induced by a short-pulse γ-irradiation of a specimen even when the initial thermostat and specimen temperature either varies within the interval where the reaction proceeds at an appreciable rate or is just fixed within this interval. Indeed one may assume that a short γ-radiation pulse produces a certain amount of stabilized active centres that enter into the reaction after being liberated.

We introduce the following dimensionless variables and parameters:

$$\begin{gathered}
\tau = \frac{t}{t_*}, \quad m = \frac{M}{M_0}, \quad n = \frac{N}{N_0}, \quad r = \frac{R}{R_*}, \\
\Theta = \frac{T - T_0}{\Delta T}, \quad t_* = \frac{c\rho V}{\alpha S}, \\
R_* = N_0\, tk_1(T_0), \quad \Delta T = \frac{R_0\, T_0^2}{E}, \\
\varepsilon = R_*\, t_*\, k(T_0), \quad \delta = t_*\, k_1(T_0), \\
p = t_*\, k_2(T_0), \quad q = R_*\, T_*\, k_3(T_0), \\
\sigma = \frac{E_1}{E}, \quad \mu = \frac{E_2}{E}, \quad \nu = \frac{E_3}{E}, \\
\beta = \frac{\Delta T}{T_0}, \quad \omega = \frac{\Omega t_*}{T_0}, \\
\xi = \frac{\varepsilon Q M}{c\rho T_0}.
\end{gathered} \tag{29}$$

Here R_0 is the gas constant. Equations (24)–(27) and the initial conditions (28) assume the forms

$$\dot{m} = -\,\varepsilon mr \exp\left(\frac{\Theta}{1 + \beta\Theta}\right), \qquad m(0) = 1, \tag{30}$$

$$\dot{n} = -\delta n \exp\left(\frac{\sigma\Theta}{1+\beta\Theta}\right), \qquad n(0) = 1, \tag{31}$$

$$\dot{r} = n\exp\left(\frac{\sigma\Theta}{1+\beta\Theta}\right) - pr\exp\left(\frac{\mu\Theta}{1+\beta\Theta}\right) - qr^2\exp\left(\frac{\nu\Theta}{1+\beta\Theta}\right), \quad r(0) = 0, \tag{32}$$

$$\dot{\Theta} = \xi mr\exp\left(\frac{\Theta}{1+\beta\Theta}\right) + \omega\tau - \Theta, \qquad \Theta(0) = 0. \tag{33}$$

To simplify the analysis, we use the $\beta = 0$ approximation [3]. We are interested in particular in the possibility of self-sustaining oscillations of Θ and the concentration r of the active species leading the process, against the background of slow variations in m and n and $\Theta_0 = \omega\tau$. For this purpose, we consider a case with small ε, δ and ω, which corresponds to a low γ-radiation dose and slow scanning of the thermostat temperature under conditions of slow active centre destabilization (see equations (29)). Investigation of the behaviour of fast variables at 'frozen' slow values is substantiated rigorously in [101] for the case when Θ and r attain steady-state values, and in [102] for processes in which Θ and r attain a stable oscillatory regime.

Equations (30)–(33) will be analysed taking into account only a monomolecular chain termination and neglecting the bimolecular chain termination, that is q is assumed to be zero in equation (32) (see equations (29)). One may similarly consider a solution for a bimolecular chain termination alone, assuming that $p = 0$ and $q \neq 0$. A qualitative analysis of the process with combined chain termination, $p \neq 0$ and $q \neq 0$, also presents no particular difficulty.

We write the fast equations (32) and (33) with due regard for the above assumptions concerning the frozen amount m of the reactant and amount n of stabilized active centres and the fixed thermostat temperature $\Theta = \omega\tau_0$:

$$\Theta = \xi mr\exp(\Theta) - (\Theta - \Theta_0), \quad r = n\exp(\sigma\Theta) - pr\exp(\mu\Theta). \tag{34}$$

5.3.1.2. *Dynamics of the fast system.* The steady-state points of equations (34) are the intersection points of zero isoclinic lines in the (Θ, r) plane:

$$r_1 = \frac{\Theta - \Theta_0}{\xi m}\exp(-\Theta), \quad r_2 = \frac{n}{p}\exp[-(\mu - \sigma)\Theta]. \tag{35}$$

The equation $r_1 = r_2$ written in terms of $x = (1 - \mu + \sigma)(\Theta - \Theta_0)$ is

$$x\exp(1-x) = \chi \equiv (1-\mu+\sigma)\frac{\xi mn}{p}\exp[1 + (1-\mu+\sigma)\Theta_0]. \tag{36}$$

It follows that the quantity χ fully determines the number of the steady-state points in equations (34). For $\chi \leqslant 0$ (which is possible solely at $1 - \mu + \sigma \leqslant 0$), the steady-state point is unique, at $0 < \chi < 1$, there exist two steady-state points while, at $\chi = 1$, they merge and disappear. No steady-state points exist for $\chi > 1$. The component Θ grows indefinitely within a finite time in this region, that is a thermal explosion occurs. Within the framework of the assumptions adopted, this phenomenon is realized when the induction period is much less than the characteristic time for variation in the quantities m, n and Θ_0. The behaviour of the integral curves of equations (34) in the regions $\chi \leqslant 0$ and $0 < \chi \leqslant 1$ depends on the type of the steady-state points, which is

well known [105] to be determined by the linearized equations for the variations $u = \Theta - \Theta$ and $v = r - r$ near the steady-state point of equations (34):

$$u = (\Theta - \Theta_0 - 1)\, u + r^{-1} (\Theta - \Theta_0)\, v,$$
$$v = (\sigma - \mu)\, pr \exp(\mu\Theta)\, u - p \exp(\mu\Theta)\, v. \tag{37}$$

The determinant D and the spur S of the matrix composed of the equation coefficients are expressed by the formulae

$$D = p \exp(\mu\Theta)(1 - x), \quad S = \Theta - \Theta_0 - 1 - p \exp(\mu\Theta), \tag{38}$$

where x is the root of equation (36), conforming to Θ: $x = (1 - \mu + \sigma)(\Theta - \Theta_0)$. It is obvious from the above relations that the saddle-type singular points correspond to values of $x > 1$ (the region where the left-hand side of equation (36) decreases) while, in the region $x < 1$ (where the function (36) is increasing), the integral curves have a focus or node ($D > 0$). Hence only one steady-state point is of the non-saddle type, namely $x \leqslant 0$ in the region $\chi \leqslant 0$, and a low-temperature steady-state ($0 < x < 1$) in the region $0 < \chi < 1$.

To answer the question of whether Θ and r may undergo self-sustaining oscillations, we find the instability region for the non-saddle-type singular point, that is the region where the conditions $S > 0$ and $D > 0$ are fulfilled simultaneously. The boundary of the instability region is calculated from the equation $S(\Theta) = 0$ (see equation (38)):

$$\Theta - \Theta_0 - 1 = p \exp(\mu\Theta), \tag{39}$$

which has either two solutions Θ_1 and Θ_2 for given parameters p, μ and Θ_0 (with the condition $S > 0$ being fulfilled at $\Theta_1 < \Theta < \Theta_2$), or none (the condition $S > 0$ may be satisfied). The condition of tangency of the left- and right-hand sides of equation (39) permits describing the region where two solutions exist by means of inequality

$$p < \frac{1}{e\mu} \exp[-\mu(\Theta_0 + 1)]. \tag{40}$$

At $\chi \leqslant 0$, we have $x \leqslant 0$ and $D > 0$, so that inequality (40) and the roots of equation (39) (Θ_1 and Θ_2) completely define the instability region for the single steady-state point. That condition $D > 0$ also holds at $\Theta = \Theta_1$ and $\Theta = \Theta_2$ means that the steady-state point is a focus near the boundary of this region and, when the representative point enters the instability region, a well known Hopf bifurcation occurs and a limiting cycle appears [19], that is Θ and r undergo self-sustaining oscillation everywhere in the instability region. Near the boundary, the oscillations are of a sine shape with a low amplitude and their frequency $\omega \approx D^{0.5}$. As the system departs from the instability boundary, the oscillations become more complicated.

When $0 < \chi < 1$, the determinant D may change its sign in the interval $\Theta_1 < \Theta < \Theta_2$ between the roots of equation (39) in the region defined by the inequality (40). Therefore the region of the non-saddle singular point should be isolated within the interval $\Theta_1 < \Theta < \Theta_2$, that is an additional condition $x = (1 - \mu + \sigma)(\Theta - \Theta_0) < 1$ should be imposed on the parameters. For convenience we rewrite this inequality in the following form:

$$\Theta - \Theta_0 - 1 < (\mu - \sigma)(\Theta - \Theta_0). \tag{41}$$

As was stated previously, this inequality introduces no restrictions other than those

imposed by conditions $S(\Theta) > 0$ at $\mu - \sigma \geqslant 1$ ($\chi \leqslant 0$). Generally speaking, at $\mu - \sigma < 1$, the inequality is not fulfilled everywhere in the interval (Θ_1, Θ_2), but only in the range

$$\Theta_1 < \Theta < \Theta_3, \quad \Theta_3 = \Theta_0 + [1 - (\mu - \sigma)]^{-1}. \tag{42}$$

It is obvious that the quantity Θ_3 decreases as $\mu - \sigma$ decreases. Moreover, when $\mu - \sigma = (\Theta_1 - \Theta_0 - 1)/(\Theta_1 - \Theta_2) > 0$, the interval (Θ_1, Θ_2) and hence the instability region for the non-saddle point disappear. When $\Theta_3 > \Theta_2$, the process is unstable provided that equation (40) is fulfilled in the interval $\Theta_1 < \Theta < \Theta_2$ as in the case when $\chi \leqslant 0$.

Near $\Theta_1 = \Theta$, the steady-state point continues to be of the focus type so that, when the representative point enters the instability region through $\Theta = \Theta$, low-amplitude periodic oscillations are generated with sustained oscillations being observed everywhere in the instability region.

Equations (34) have a stable limit cycle on the (Θ, r) phase plane everywhere in the instability region of a point of the node or focus type, that is the solution is periodic in time (self-sustaining). The existence of the limiting cycle is ensured by the fact that there always is some trajectory representing a solution to the fast equations and missing the steady-state point that the considerations and constructions [103] are also applicable. It should also be noted that the finite solutions of the fast equations will be obvious if one assumes that the exponents are finite ($\beta \neq 0$ in equations (32) and (33)).

5.3.1.3. *Dynamics of the full set of equations (30)–(33).* When m and n are depleted slowly and the temperature Θ_0 is scanned at a low rate, the phase portrait of the integral curves of the fast equations (34) alters slowly. At the initial instant (with the characteristic time of the slow process) $\Theta_0 = 0$, for $\chi \leqslant 0$, the fast solution remains in the same region with the only steady-state point during the entire process. Evolution of the solution may change only the type of the steady-state point (from a node to a focus or vice versa) and its stability. The loss of the stability leads to sustained oscillations, whose amplitude varies with m, n and Θ_0. With decreasing m and n and increasing Θ_0 the oscillations may disappear, and the steady-state point becomes stable again. At $\chi > 1$, the specimen temperature first rises; this may be interpreted as a thermal explosion, as has been mentioned above. Depletion of reactant (indicated by m) and of the stabilized active centres (indicated by n) shifts the fast solution to the region with two steady-state points $0 < \chi < 1$ and the fast variables Θ and r attain the low-temperature quasisteady state. Then the fast system passes the region of self-sustaining oscillations, provided that conditions (40) and (42) are fulfilled and reaches the final state, in which the specimen temperature is equal to that of the thermostat when the reactant and the stabilized active centres are completely depleted. In this final state, either no active centres are present in the specimen or their concentration is determined by the rate of their escape from the radiation traps if the active centres have been produced in excess and none of them has been consumed during the reaction.

5.3.2. *Radiation-induced post-polymerization of crystalline heptylacrylate*

To illustrate application of the aforesaid theoretical considerations, we discuss the results of the studies on the polymerization of crystalline heptylacrylate specimens subjected to γ-radiation at 77 K during their heating in both the sustained oscillatory and non-oscillatory regimes. On being quickly cooled to 77 K, heptylacrylate monomer vitrifies completely. Heating of these specimens in a calorimeter allows observation of their transition from a glassy state to a supercooled liquid (devitrification temperature $T = 138$ K), crystallization of the supercooled liquid in the

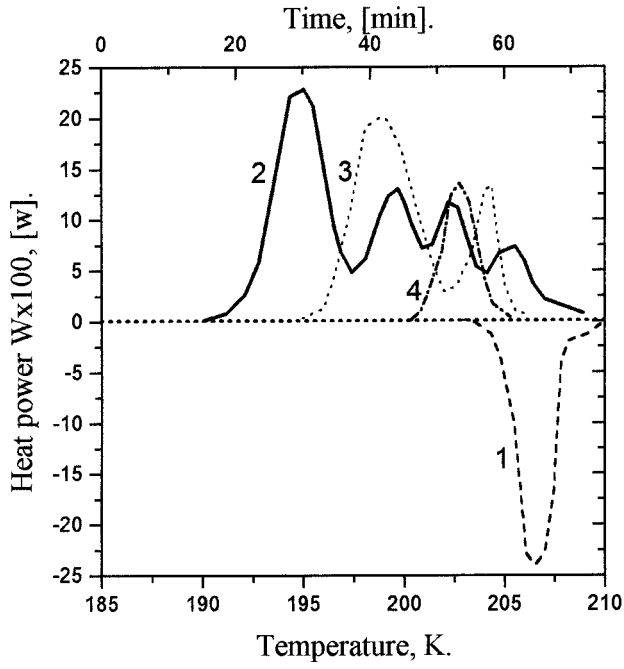

Figure 9. A calorimetric curve of unirradiated heptylacrylate defreezing (curve 1) and variations in the heat release rate on heating the γ-irradiated heptyl acrylate with doses of 100 kGy (curve 2), 17.5 kGy (curve 3) and 5 kGy (curve 4) at 77 K.

temperature range 140–205 K and then melting of the monomer crystallites at 205–210 K. However, if the monomer is annealed at 205 K and then is cooled to 77 K, the heptylacrylate transforms completely into the crystalline state. The calorimetric heating curves of such specimens exhibit only an endothermic peak of monomer melting at $T = 208$ K (figure 9, curve 1). It is these specimens that have been used in the post-polymerization studies.

To accumulate the active polymerization centres, monomers were irradiated at 77 K (5–100 kGy). The calorimetric heating curves for pre-irradiated specimens are presented in figure 9 (curves 2–4). It is seen that the polymerization reaction, as detected from the heat release, starts at temperatures that are 15–20 K lower than the monomer melting point at which the translating mobility of the molecules becomes unfrozen.

The polymerization rate depends strongly on the temperature in the initial portion of the kinetic curve and rapidly reaches its maximal value. Then, it decreases sharply and then grows again. In the final run, several periods of reaction acceleration and deceleration are observed. The reaction rate oscillations are of a spasmodic nature. Any increases in the γ-radiation dose shifts the beginning of the process towards lower temperatures and increases the amplitude of rate oscillations (cf. curves 2 and 3). At sufficiently small ϕ-irradiation doses no post-polymerization rate oscillations are observed any longer (curve 4). Analogous oscillations of the polymerization rate were also observed with another acrylic monomer, methyl methacrylate [98].

The mathematical model of the post-polymerization process suggests in the present work allows one to explain qualitatively the observed behaviour of the radiation-induced post-polymerization of crystallin heptylacrylate. Indeed, when the

γ-irradiation dose is small, the steady-state point of the fast solution to equations (34) is located on the increasing portion of the r curve and is stable. In these conditions, two stages of the process may be determined. First the trajectory of the fast solution is attracted to this steady-state point, and the specimen temperature increases appreciably above that of the thermostat. Then the trajectory is captured by the stable steady-state point and follows it until the reaction stops owing to depletion of the stabilized active centres.

When the irradiation dose is large enough (figure 9, curves 2 and 3), the post-polymerization process may be divided into four stages. First the heat release increases very rapidly, and this growth may be interpreted as a thermal explosion in the sense mentioned above. Next the trajectory is captured by the stable steady-state point of the fast equations and moves together with it. Later on the trajectory enters the region of sustained oscillations near the unstable steady-state point. After the trajectory leaves the region of sustained oscillations, it is again captured by the steady-state point of the fast equations and moves together with this point until the reaction is completed.

Further investigations of the dynamics and kinetic parameters will permit a detailed description of the post-polymerization reaction behaviour.

5.3.3. *Determination of the rate constants in the steady-state reaction regime*

In all the cases considered above, the reaction is completed in a steady-state regime, in which the fast variables (the specimen temperature Θ and the amount r of the active centres leading the reaction) are adjusted to the instantaneous magnitudes of the slow variables (the amount m of the reactant, the amount n of the stabilized active centres and thermostat temperature Θ_0). This allows information to be obtained about the unknown constants of the post-polymerization reaction. As has been mentioned above, the process can be completed in two different regimes depending on what is depleted first, the active centres or the reactant.

Let us assume that the active centres are depleted first. Under these conditions the amount of the reactant tends to a certain final value m_f and the specimen temperature approaches the thermostat temperature Θ_0. The amount of the active centres diminishes continuously while the reaction dynamics are governed by the equation (see equation (34))

$$\dot{r} \approx -pr \exp(\mu\Theta_0), \tag{43}$$

which yields

$$r(\tau) \approx r_0 \exp\{-[p \exp(\mu\Theta_0)]\,\tau\}. \tag{44}$$

The parameter measured in the experiment is the heat release rate w, which is proportional to the rate of reactant consumption:

$$w = -\dot{m} = g(\tau). \tag{45}$$

From equation (30), one obtains

$$g(\tau) \approx \varepsilon m_f \exp(\Theta_0)\, r_0 \exp\{-[p \exp(\mu\Theta_0)]\,\tau\}, \tag{46}$$

and

$$\ln[g(\tau)] \approx \ln[\varepsilon m_f \exp(\Theta_0)\, r_0] - p \exp(\mu\Theta_0)\,\tau. \tag{47}$$

The dependence of $\ln g$ on time τ tends asymptotically to a certain straight line towards the completion of the reaction. The slope of this line, $\tan(\phi)$, is

$$\tan(\phi) = p \exp(\mu\Theta_0). \tag{48}$$

It should be noted here that scanning of the thermostat temperature must be terminated when measuring the heat release at the end of the reaction and the temperature must be fixed at Θ_0. However, two more parameters are unknown in equation (48), namely p and μ. To determine these, one has to perform measurements at various fixed thermostat temperatures Θ_0. In doing so, one may not control the γ-irradiation dose, but it should not be too large so as not to deplete fully the reactant. When these measurements have been accomplished, one may plot the $\ln[\tan(\phi)]$ versus Θ_0 dependence and derive the equation of the asymptotic straight line $A + \Theta_0 \tan(\phi)$ that yields $\mu = \tan(\phi)$ and $p = \exp(A)$.

One can thus measure the parameters characterizing the rate and activation energy for destruction of the principal active centres. The case when the initial reactant is depleted first and the reaction near its termination is controlled by the amount of the reactant left may be analysed in a similar way.

5.3.4. *Regimes of post-radiation polymerization during devitrification*

Oscillatory regimes of low-temperature radiation-induced solid-phase reactions were observed for post-polymerization during devitrification of the matrix. For example, we consider oscillations of the chain polymerization reaction rate in the system being devitrified. Post-radiation acetaldehyde polymerization in a glassy butyl chloride matrix is investigated.

A solution of acetaldehyde in butyl chloride (a molar ratio of about 1:4) vitrifies completely when cooled to 77 K. Upon heating of the system in a calorimeter, a transition of the glassy state to the supercooled liquid (devitrification) is observed within the temperature range 94–97 K; the liquid then crystallizes (at 112–115 K) and thereupon melts ($T = 145$ K).

The same system pre-irradiated at 77 K with γ-rays shows some exothermicity in the devitrification region when being heated. This heat release is due to acetaldehyde polymerization. Depending on the heat losses from the calorimetric cell, different regimes of the reaction are possible.

The process may occur without any detectable temperature rise in the cell with respect to the calorimeter body (steady-state regime). Realization of the steady-state regime requires sufficiently intense heat transfer from the reaction cell. This can be achieved in the experiment by varying some parameters, namely

(1) by decreasing the rate of specimen heating,
(2) by enhancing the heat losses, e.g. by increasing the surface-area-to-volume ratio of the specimen (decreasing the original specimen weight) and
(3) by decreasing the dose of γ-radiation, which lowers the concentration of the stabilized active centres in the system, that is reduces the rate of heat release owing to polymerization reaction.

The rate of acetaldehyde post-polymerization increases as the temperature rises during the reaction (provided that the specimen in the cell is not excessively overheated), reaches its maximum and then decays gradually owing to the depletion of the monomer and active centres generated by radiation (figure 10, curve 1). The initial, that is increasing, portion of the calorimetric curve can be fairly well represented by a straight line in the Arrhenius coordinates with the energy $E \approx 25$ kJ mol^{-1}.

The thermal explosion regime represents the opposite extreme case. An explosion occurs when the heat losses from the cell become less intense, which is caused by

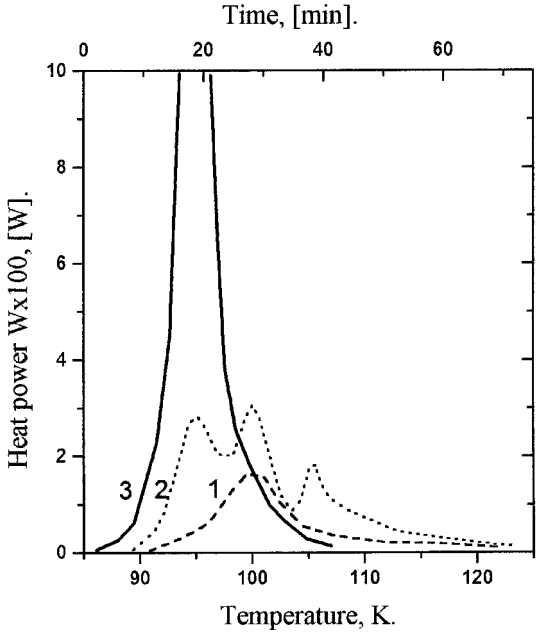

Figure 10. Variations in the heat release rate in the devitrification region of acetaldehyde (AA) post-polymerization in the matrix of butyl chloride (BC) for the samples: curve 1, 0.097 g of AA + 0.367 g of BC; curve 2, 0.138 g of AA + 0.549 g of BC; curve 3, 0.175 g of AA + 0.672 g of BC. The doses of γ-pre-irradiation at 77 K are 120 kGy and 300 kGy for curve 3. T is the temperature of the calorimeter block.

increasing the weight of a specimen, the rate of its heating and the radiation dose (curve 3 of figure 10).

An oscillatory regime of the process was observed when the heat transfer from a specimen was of intermediate intensity. Several cycles of the reaction rate growth and decay were observed in the experiments (curve 2 of figure 10).

It follows that, depending on the conditions in which the reaction is conducted, the behaviour of the system is different. There are three main regimes of the process: a steady-state regime, occurring without an appreciable temperature rise in the specimen, a thermal explosion and an oscillatory regime. An analysis of these first experimental data allows us to draw the conclusion that the oscillation observed in the system studied may be accounted for by a thermokinetic mechanism. The following relationships may be suggested for a rough estimation of the boundaries of the region where the oscillatory regimes are realized: $T_t < T_c < T_t + \Delta T$ and $\tau > n\tau_{os}$. Here T_c is the temperature rise (over the thermostat temperature T_t) in the mixture reacting in the oscillatory regime, ΔT is the pre-explosion temperature rise ($\Delta T = RT^2/E$), τ is the mean lifetime of the active centres ($\tau = 1/k$ and $\tau = 1/kR$ for monomolecular decay and bimolecular decay respectively of the active centres, k is the rate constant of active centres' decay and R is the initial concentration of the active polymerization centres), τ_{os} is the period of oscillations and n is the number of oscillation cycles.

It is natural that the dynamics of the decay of radicals accumulated in the sample in low-temperature radiolysis are different in different reaction regimes. Figure 11 gives, as an example, the dynamics of the change in the radical concentration with a temperature rise for a glassy solution of acrylic acid in ethanol radiolysed at 77 K. An

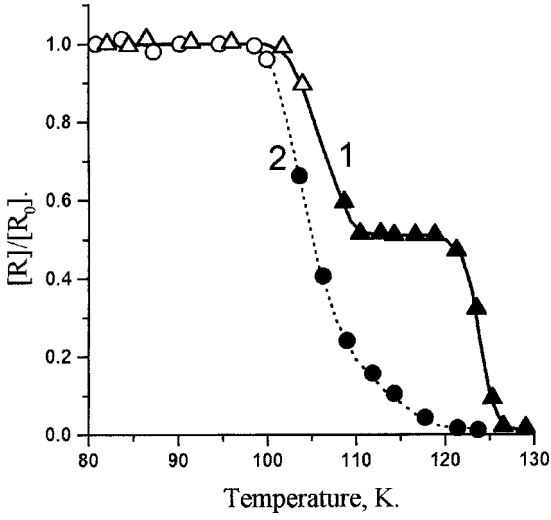

Figure 11. Variations in the relative radical concentration during the heating of 17% solutions of acrylic acid in ethanol irradiated at 77 K with doses of 20 kGy (curve 1) and 50 kGy (curve 2). The rates of sample heating are 0.2 K min^{-1} for curve 1 and 0.5 K min^{-1} for curve 2. The concentrations of the propagating polymer chains are shown as full symbols.

effective post-polymerization in this system is recorded in the temperature region of the softening matrix.

In the case of the steady-state reaction (the absence of marked overheating in a sample), the growing macroradical in the range 110–120 K does not recombine and only propagation of the polymer chains occurs (figure 11, curve 1). On disturbing the quasi-isothermal regime and origination of post-polymerization rate oscillations, the growing macroradicals (figure 11, curve 2) decay quite effectively. Finally, at high rates of system heating (about 600 K min^{-1}) no propagating polymer chains are formed at all because of the decay of active centres in the early stages.

Summarizing the investigation results given in this section we should note that various regimes of carrying out chemical conversion are of interest in view of the possibility of increasing the selectivity of complex processes and widening the scope of controlling the cryochemical synthesis. Usually, the thermal non-uniformity arising during the operation of chemical reactors is an unwanted side effect, resulting in a reduction in the quality of products and possible emergencies. The understanding of the mechanism of the process allows us to suppress the auto-oscillations and maintain the steady-state regime. However, the auto-oscillation regimes may also prove favourable, ensuring a much higher yield of products on average than the steady-state regime. Such advantages are especially pronounced when the target product is an intermediate compound in a complicated chain chemical conversion [106].

As an example of the influence of different reaction regimes on the properties of the final product, let us examine the radiation-induced cryopolymerization of 1,3-bis(dimethylamino)isopropyl methacrylate. This polymer product is employed to achieve special goals in biomedicine and ecology [107]. Depending on the conditions of heat removal from the reaction volume, different regimes of matrix devitrification were realized: steady-state regime or oscillatory regime and thermal explosion.

The dependence of an average molecular mass of the polymer on the dose of pre-irradiation at different regimes of post-polymerization is shown in figure 7. In the case

of the auto-oscillation regimes of polymerization the molecular mass M_W of the polymer decreases from 2.8×10^6 to 1.4×10^6 with an increase in the pre-irradiation dose from 10 to 118 kGy. In the case of the steady-state polymerization, M_W decreases from 1.5×10^6 to 0.3×10^6. An appreciable rise in the molecular mass in passing from the steady-state regime to the oscillatory regime is evidently due to the increased molecular mobility of the propagating polymer chains under conditions of local overheating, and hence a predomination of their bimolecular termination. The increase in the molecular mass is connected with this fact.

The regime of thermal explosion leads to a polymer with a different supermolecular structure that is characterized by its microheterogeneity [107]. A more detailed analysis of the polymeric products obtained in this series of experiments has shown the non-steady state in the process of low-temperature polymerization (oscillatory regime and thermal heat explosion) to lead to widening of molecular mass polymer distribution toward high molecular masses.

This review is addressed to a wide circle of readers. Scientists and researchers dealing with the theory of chemical reactivity, cosmochemistry, chemistry of solids and macromolecular chemistry will find in it some new ideas.

References

[1] Kolschutter, H. W., and Sprenger, L., 1932, *Z. phys. Chem.*, **16**, 282.
[2] Travers, M. S., 1936, *Trans. Faraday Soc.*, **32**, 246.
[3] Letort, M., 1936, *C. r. hebd. Séanc. Acad. Sci., Paris*, **202**, 767.
[4] Kiryukhin, D. P., Kaplan, A. M., Barkalov, I. M., and Goldanskii, V. I., 1972, *Visokomolek. Soed.* A, **14**, 2115.
[5] Goldanskii, V. I., Trakhtenberg, L. I., and Flerov, V. N., 1986, *Tunnel Phenomena in Chemical Physics* (Moscow Nauka), p. 296.
[6] Ovchinnikova, M. Ya., 1979, *Chem. Phys.*, **36**, 85.
[7] Benderskii, V. A., Goldanskii, V. I., and Ovchinnikov, A. A., 1980, *Chem. Phys. Lett.*, **73**, 492.
[8] Trakhtenberg, L. I., Klochikhin, V. L., and Pshezhetzky, S. Ya., 1981, *Chem. Phys.*, **59**, 191, 1982, *ibid.*, **69**, 121.
[9] Benderskii, V. A., Makarov, D. E., and Wight, C. A., 1994, *Chemical Dynamics at Low Temperature* (New York: Wiley Interscience).
[10] Barelko, V. V., Barkalov, I. M., Gol'danskii, V. I., Kiryukhin, D. P., and Zanin, A. M., 1988, *Adv. chem. Phys.*, **74**, 339.
[11] Barelko, V. V., Barkalov, I. M., Gol'danskii, V. I., Kiryukhin, D. P., and Zanin, A. M., 1990, *Russ. chem. Rev.*, **59**, 205.
[12] Semenov, N. N., 1960, *Khim. Tekhnol. Polimerov*, (7–8), 196.
[13] Adirovich, E. I., 1961, *Dokl. Akad. Nauk SSSR*, **136**, 117.
[14] Magat, M., 1962, *Polymer*, **3**, 449.
[15] Chapiro, A., 1964, *J. Polym. Sci.* C, **4**, 1551.
[16] Kargin, V. A., and Kabanov, V. A., 1964, *Zh. Vses. Khim. Obstich. D. I. Mendeleev*, **9**, 602.
[17] Goldanskii, V. I., and Enikolopian, N. S., 1966, *Radiation Chemistry of Polymers* (Nauka: Moscow), pp. 7–15.
[18] Abkin, A. D., Scheinker, A. P., and Gerasimov, G. N., 1973, *Radiation Chemistry of Polymers* (Nauka: Moscow), p. 7.
[19] Goldanskii, V. I., 1975, *Russ. chem. Rev.*, (12).
[20] Kaplain, A. M., Kiryukhin, D. P., Barkalov, I. M., and Goldanskii, V. I., 1970, *Dokl. Acad. Nauk SSSR*, **190**, 1387.
[21] Michailov, I, Bolschakov, A. I., Lebedev, Ya. S., and Goldanskii, V. I., 1972, *Fiz, tverd, Tela*, **14**, 1172.
[22] Kiryukhin, D. P., Kaplan, A. M., Barkalov, I. M., and Goldanskii, V. I., 1970, *Visokomolek. Soed.* B, **12**, 491.

[23] KIRYUKHIN, D. P., KAPLAN, A. M., BARKALOV, I. M., and GOLDANSKII, V. I., 1971, *Dokl. Akad. Nauk SSSR*, **199**, 857.
[24] KIRYUKHIN, D. P., KAPLAN, A. M., BARKALOV, I. M., and GOLDANSKII, V. I., 1972, *Dokl. Akad. Nauk SSSR*, **206**, 147.
[25] KIRYUKHIN, D. P., KAPLAN, A. M., BARKALOV, I. M., and GOLDANSKII, V. I., 1973, *Dokl. Akad. Nauk SSSR*, **211**, 632.
[26] GOLDANSKII, V. I., FRANK-KAMENETSKII, M. D., and BARKALOV, I. M., 1973, *Dokl. Akad. Nauk SSSR*, **211**, 133.
[27] GOLDANSKII, V. I., FRANK-KAMENETSKII, M. D., and BARKALOV, I. M., 1973, *Science*, **182**, 1344.
[28] KIRYUKHIN, D. P., BARKALOV, I. M., and GOLDANSKII, V. I., 1974, *Visokomolek. Soed.* B, **16**, 565.
[29] GOLDANSKII, V. I., KIRYUKHIN, D. P., and BARKALOV, I. M., 1974, *Khim. visokich Energii* (*High Energy Chem.*), **8**, 279.
[30] SERGEEV, G. B., and SHVEDCHIKOV, A. P., 1964, *Zh. Vses. Khim. Obstich. D. I. Mendeleev*, **9**, 602.
[31] SERGEEV, G. B., and BATIUK, V. A., 1978, *Cryochemistry* (Moscow: Khimia), p. 296.
[32] KIRYUKHIN, D. P., BARKALOV, I. M., and GOLDANSKII, V. I., 1978, *Dokl. Akad. Nauk SSSR*, **238**, 388.
[33] ZANIN, A. M., KIRYUKHIN, D. P., BARKALOV, I. M., and GOLDANSKII, V. I., 1980, *Dokl. Akad. Nauk SSSR*, **253**, 142.
[34] CALVIN, M., 1969, *Chemical Evolution* (Oxford University Press).
[35] SANCHEZ, M. A., FERRIS, J. P., and ORGEL, L. E., 1966, *Science*, **154**, 784.
[36] FERRIS, J. P., and EDELSON, E. H., 1978, *J. org. Chem.*, **43**, 3989.
[37] FERRIS, J. P., JOSHI, P. C., EDELSON, E. H., and LAWLESS, J. G., 1978, *J. molec. Evolution*, **11**, 293.
[38] FERRIS, J. P., and HAGAN, W. J., 1984, *Tetrahedron*, **40**, 1093.
[39] STAHLER, S. W., 1984, *Astrophys. J.*, **281**, 209.
[40] MEISSE, C., ARAKAWA, E. T., KHARE, B. N., THOMPSON, W. R., and SAGAN, C., 1991, *Bull. Am. Astron. Soc.*, **23**, 1189.
[41] SAGAN, C., and CYBA, C. F., 1991, *Bull. Am. Astron. Soc.*, **23**, 1211.
[42] MOZHAEV, P. S., KIRYUKHIN, D. P., KICHIGINA, G. A., and BARKALOV, I. M., 1993, *Mendeleev Commun.*, 64.
[43] MOZHAEV, P. S., KIRYUKHIN, D. P., KICHIGINA, G. A., and BARKALOV, I. M., 1995, *Khim. visokich Energii* (*High Energy Chemistry*), **29**, 19.
[44] MOZHAEV, P. S., KIRYUKHIN, D. P., KICHIGINA, G. A., ALIEV, Z. G., ATOVMIAN, L. O., and BARKALOV, I. M., 1994, *Dokl. Akad. Nauk SSSR*, **335**, 747.
[45] KLISS, R. M., and MATTHEWS, C. N., 1962, *Proc. natn. Acad. Sci. USA*, **48**, 1300.
[46] MOSER, R. E., ERITSCH, J. M., WESTMAN, T. L., KLISS, R. M., and MATTHEWS, C. N., 1967, *J. Am. chem. Soc.*, **89**, 5673.
[47] BARKALOV, I. M., GOLDANSKII, V. I., and ENIKOLOPIAN, N. S., 1962, *Dokl. Akad. Nauk SSSR*, **147**, 396.
[48] CHAPIRO, A., 1967, *Chimia*, **21**, 454.
[49] CHAPIRO, A., JENDRYCHOWSKA-BONAMOUR, A. M., and PEREC, L., 1968, *Adv. Chem.*, **82**, 513.
[50] GUSAKOVSKAJ, I. G., NIKOLSKII, V. G., and GOLDANSKII, V. I., 1970, *Khim. visokich Energii* (*High Energy Chem.*), **7**, 434.
[51] KIM, I. P., KAPLAN, A. M., BARKALOV, I. M., and GOLDANSKII, V. I., 1971, *Dokl. Akad. Nauk SSSR*, **178**, 164.
[52] GEORGIEV, G. S., KAPLAN, A. M., ZUBOV, V. P., and BARKALOV, I. M., 1973, *Visokomolek. Soed.* A, **14**, 177.
[53] BOLSHAKOV, A. I., MIKHAYLOV, A. I., BARKALOV, I. M., and GOLDANSKII, V. I., 1972, *Dokl. Akad. Nauk SSSR*, **205**, 379.
[54] BOLSHAKOV, A. I., MIKHAYLOV, A. I., and BARKALOV, I. M., 1973, *Teor. éksp. Khim.* **9**, 831.
[55] STUKAN, R. A., ARCHIPOV, I. L., ROCHEV, V. JA., BOLSHAKOV, A. I., and BARKALOV, I. M., 1986, *Visokomolek. Soed.* A, **28**, 1446.
[56] BOLSHAKOV, A. I., and BARKALOV, I. M., 1981, *Visokomolek. Soed.* A, **23**, 1086.
[57] BOLSHALOV, A. I., BARKALOV, I. M., and GOLDANSKII, V. I., 1980, *Dokl. Akad. Nauk SSSR*, **255**, 367.

[58] Muidinov, M. R., Barkalov, I. M., Kiryukhin, D. P., and Kichigina, G. A., 1983, *Visokomolek. Soed.* A, **25**, 818.
[59] Barkalov, I. M., Kiryukhin, D. P., and Kichigina, G. A., 1984, *Eur. Polym. J.*, **20**, 1013.
[60] Meleshevich, A. P., 1970, *Usp. Khim.*, **39**, 444.
[61] Kichigina, G. A., Muidinov, M. R., Kiryukhin, D. P., and Barkalov, I. M., 1983, *Khim. visokich Energii* (*High Energy Chem.*), **17**, 249.
[62] Djagtspanian, R. V., and Filipov, M. T., 1973, *Radiatsionnaya Khimiya Galogensoderjzhashchikh Organicheskikh Soedinenii* (Moscow: Atomizdat).
[63] Kiryukhin, D. P., Barkalov, I. M., and Goldanskii, V. I., 1977, *Khim. visokich Energii* (*High Energy Chem.*), **11**, 438.
[64] Sergeev, G. B., and Batiuk, V. A., 1978, *Kriokhimiya* (*Cryochemistry*) (Moscow: Khimiya), p. 296 (in Russian).
[65] Kiryukhin, D. P., Barkalov, I. M., and Goldanskii, V. I., 1979, *J. chem. Phys.*, **76**, 1013.
[66] Zanin, A. M., Kiryukhin, D. P., Barelko, V. V., and Barkalov, I. M., 1982, *Khim. Fiz.*, **1**, 265.
[67] Barelko, V. V., Barkalov, I. M., Vaganov, D. A. and Kiryukhin, D. P., 1983, *Khim. Fiz.*, **2**, 980.
[68] Zeldovich, Ya. B., Barenblatt, G. I., Librovich, V. I., and Makhviladze, G. M., 1980, *Mathematical Theory of Combustion and Explosion* (Moscow: Nauka), p. 363.
[69] Zanin, A. M., Kiryukhin, D. P., Nikol'skii, V. S., Barelko, V. V., and Barkalov, I. M., 1983, *Izv. Akad. Nauk SSSR, Ser. Khim.*, (6), 1228.
[70] Kiryukhin, D. P., Zanin, A. M., Barelko, V. V., and Barkalov, I. M., 1986, *Dokl. Akad. Nauk SSSR*, **288**, 406.
[71] Kichigina, G. A., Zanin, A. M., Kiryukhin, D. P., and Barkalov, I. M., 1988, *Khim. Fiz.*, **7**, 543.
[72] Barkalov, I. M., Goldanskii, V. I., Zanin, A. M., and Kiryukhin, D. P., 1987, *Dokl. Akad. Nauk SSSR*, **296**, 891.
[73] Zanin, A. M., Kiryukhin, D. P., Barelko, V. V., and Barkalov, I. M., 1983, *Dokl. Akad. Nauk SSSR*, **268**, 1146.
[74] Kiryukhin, D. P., Mozaev, P. S., and Barelko, V. V., 1992, *Khim. Fiz.*, **11**, 264.
[75] Harner, W. E., and Hailes, H. R., 1933, *Proc. R. Soc.*, **139**, 576.
[76] Delmon, B., 1972, *Kinetika Geterogennykh Reaktsii* (Moscow: Mir).
[77] Rayevskii, A. V., and Manelis, G. B., 1963, *Dokl. Akad. Nauk SSSR*, **155**, 886.
[78] Rayevskii, A. V., Manelis, G. B., Boldyrev, V. V., and Votinova, L. A., 1965, *Dokl. Akad. Nauk SSSR*, **160**, 1136.
[79] Manelis, G. B., 1979, *Problemi Khimicheskoii Kinetiki* (Moscow, Nauka), p. 266.
[80] Manelis, G. B., Rubtsov, Yu. I., and Rayevskii, A. V., 1970, *Fiz. goreniya Vzryva*, **6**, 3.
[81] Rayevskii, A. V., 1981, *Mechanisms of Thermal Decomposition of Ammonium Perchlorate* (Chernogolovka), p. 30.
[82] Benderskii, V. A., Misochko, E. Ya., Ovchinnikov, A. A., and Philippov, P. G., 1980, *Pisma Zh. éksp. teor. Fiz.*, **32**, 429.
[83] Benderskii, V. A., Misochko, E. Ya., Ovchinnikov, A. A., and Philippov, P. G., 1982, *Khim. Fiz.*, **1**, 685.
[84] Benderskii, V. A., Misochko, E. Ya., Ovchinnikov, A. A., and Philippov, P. G., 1983, *Zh. Fiz. Khim.*, **57**, 1079.
[85] Rigel, V. R., Slutsker, A. I., and Tomashevskii, E. E., 1974, *Kineticheskaya Priroda Prochnosti Tverdich Tel* (Moscow: Nauka), p. 560.
[86] Meade, C., and Jeanloz, R., 1989, *Nature*, **339**, 616.
[87] Zhabotinskii, A. M., 1974, *Oscillations of Concentrations* (Moscow: Nauka).
[88] Nicolis, G., and Prigogine, I., 1977, *Self-Organization in Non-equilibrium Systems* (New York: Wiley–Interscience).
[89] Frank-Kamenetskii, D. A., 1967, *Diffusion and Heat Transfer in Chemical Kinetics* (Moscow: Nauka).
[90] Haken, H., 1987, *Advanced Synergetics*, Springer Series in Synergetics, Vol. 20, second corrected printing (Berlin: Springer).
[91] Fiold, R. I., and Burger, M. (editors), 1985, *Oscillation and Travelling Waves in Chemical Systems* (New York: Wiley).
[92] Volter, B. V., and Sal'nikov, I. E., 1981, *Stability Regimes of Chemical Reactors* (Moscow: Khimia).

[93] KIRYUKHIN, D. P., and BARKALOV, I. M., 1983, *Khim. visokich Energii* (*High Energy Chem.*), **17**, 301.
[94] KIRYUKHIN, D. P., NEFEDOV, B. A., and KHUDYAEV, S. I., 1986, *Dokl. Akad. Nauk SSSR*, **291**, 1406.
[95] NEFEDOV, B. A., KIRYUKHIN, D. P., BOL'SHAKOV, A. I., and KHUDYAEV, S. I., 1987, *Khim. Fiz.*, **6**, 813.
[96] KIRYUKHIN, D. P., KICHIGINA, G. A., and BARKALOV, I. M., 1988, *Khim. Fiz.*, **7**, 864.
[97] BOL'SHAKOV, A. I., KIRYUKHIN, D. P., and BARKALOV, I. M., 1989, *Visokomolek. Soed.* B, **31**, 219.
[98] KIRYUKHIN, D. P., 1990, *Chemistry of Low-temperature and Cryochemical Technology* (Moscow: MGU), pp. 27–32.
[99] SAL'NIKOV, I. E., 1948, *Dokl. Akad. Nauk SSSR*, **60**, 405.
[100] SAL'NIKOV, I. E., 1949, *J. phys. Chem.* (*Russ.*), **23**, 258.
[101] TIKHONOV, A. N., 1952, *Mat. Sb.*, **31**, 575.
[102] PONTRYAGIN, L. S., and RODYGIN, L. V., 1960, *Dokl. Akad. Nauk SSSR*, **131**, 255.
[103] PONTRYAGIN, L. S., 1970, *Ordinary Differential Equations* (Moscow: Nauka).
[104] MARSDEN, J. E., and MCCRACKEN, M., 1976, *The Hopf Bifurcation and its Applications* (Berlin: Springer).
[105] BAUTIN, N. N., and LEONTOVICH, E. A., 1976, *Metidi i Priemi Kachestvennogo Issledovania Dinamicheskih Sistem na Ploskosti* (Moscow: Nauka).
[106] DOUGLAS, I. M., and GAITONDE, N. Y., 1967, *Ind. Engng Chem., Fundamentals*, **6**, 265.
[107] BONDARENKO, S. JU., KIRYUKHIN, D. P., and USHAKOVA, V. N., 1990, *Proceedings of the Second USSR Conference on Theoretical and Industrial Chemistry*, Obninsk, 1990 (Moscow: Nauka), p. 35.